# *The active-layer hydrology of a peat plateau with thawing permafrost (Scotty Creek, Canada)*

**W. L. Quinton & J. L. Baltzer**

**Hydrogeology Journal**
Official Journal of the International Association of Hydrogeologists

ISSN 1431-2174
Volume 21
Number 1

Hydrogeol J (2013) 21:201-220
DOI 10.1007/s10040-012-0935-2

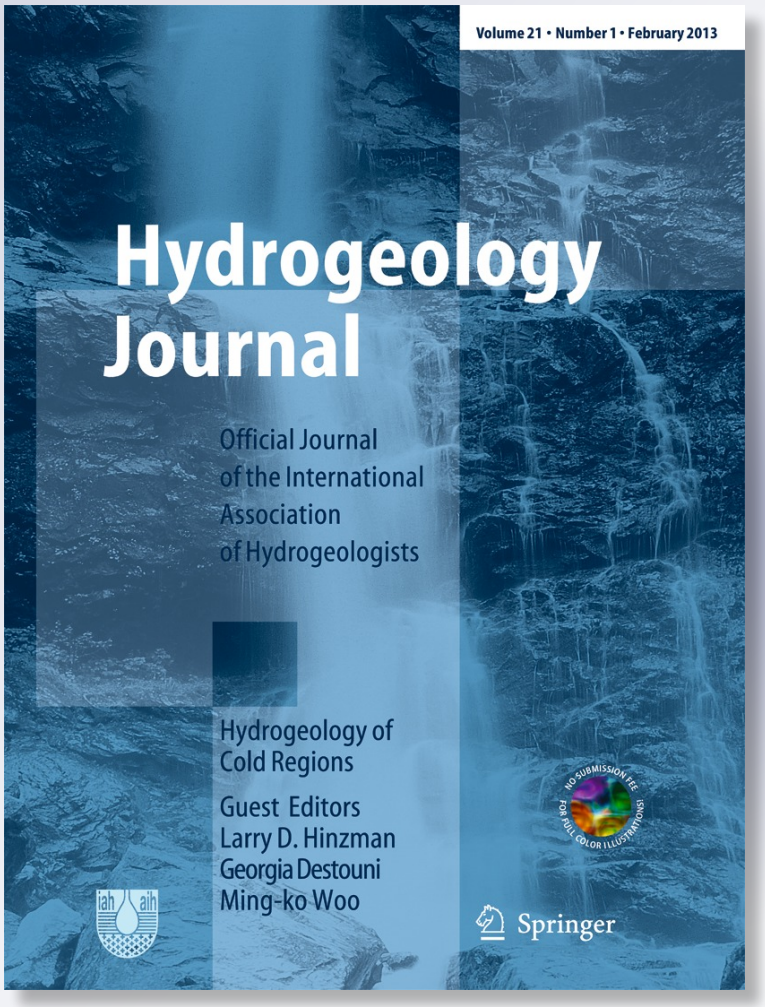


Springer

# The active-layer hydrology of a peat plateau with thawing permafrost (Scotty Creek, Canada)

W. L. Quinton · J. L. Baltzer

**Abstract** The southern margin of permafrost is experiencing unprecedented rates of thaw, yet the effect of this thaw on northern water resources is poorly understood. The hydrology of the active layer on a thawing peat plateau in the wetland-dominated zone of discontinuous permafrost was studied at Scotty Creek, Northwest Territories (Canada), from 2001 to 2010. Two distinct and seasonally characteristic levels of unfrozen moisture were evident in the 0.7-m active layer. Over-winter moisture migration produced a zone of high ice content near the ground surface. The runoff response of a plateau depends on which of the three distinct zones of hydraulic conductivity the water table is displaced into. The moisture and temperature of the active layer steadily rose with each year, with the largest increases close to the ground surface. Permafrost thaw reduced subsurface runoff by (1) lowering the hydraulic gradient, (2) thickening the active layer and, most importantly, (3) reducing the surface area of the plateau. By 2010, the cumulative permafrost thaw had reduced plateau runoff to 47% of what it would have been had there been no change in hydraulic gradient, active layer thickness and plateau surface area over the decade.

**Keywords** Permafrost · Hydrology · Wetlands · Runoff · Canada

## Introduction

North-western Canada is one of the most rapidly warming regions on Earth (Johannessen et al. 2004), and permafrost thaw is one of the most important and dramatic manifestations of climate warming in this region (Jorgenson et al. 2010). While permafrost thaw occurs in varying degrees throughout the North, it is the southern boundary of permafrost where the rates of thaw are the greatest. For example, 30–65 % of permafrost on the southern margins of the discontinuous zone in north-western Canada has degraded over the last 100–150 years (Beilman and Robinson; 2003), with rates of degradation increasing in recent decades (e.g. Lantz and Kokelj 2008; Quinton et al. 2011). Moreover the southern boundary itself migrated northward by about 120 km between 1964 and 1990 (Kwong and Gan; 1994). As part of the Kwong and Gan (1994) study, a detailed trend analyses was conducted which demonstrated that the disappearance of permafrost is largely the result of climate warming, that the region experienced a general warming trend for the period 1949–1989, and that this warming was most prominent in the minimum temperature series. The high rate of migration reported by Kwong and Gan (1994) is possible because the permafrost of this region is (1) discontinuous, and therefore its thaw is driven by both horizontal heat flows from the permafrost edges and vertical heat flows from the ground surface; (2) relatively warm, and therefore the energy required for permafrost thaw is lower than at higher latitudes; and (3) relatively thin (<10 m).

Region-wide warming on the spatial and temporal scale identified by Kwong and Gan (1994) has brought about system-wide responses as described by Rowland et al. (2010). One such response is a significant expansion of permafrost-free terrain over the last several decades along the southern permafrost boundary (e.g. Thie 1974; Beilman and Robinson 2003) where ice-rich permafrost in the form of tree-covered peat plateaus occurs as islands within a wetland-dominated treeless terrain of flat bogs, channel fens and other wetlands. Climate warming has introduced an imbalance to the cycle of permafrost aggradation and degradation described by Zoltai (1993) such that permafrost degradation and wetland formation is favoured. As permafrost thaws, the plateau ground surfaces subside and become engulfed by their neighbouring wetlands (Jorgenson and Osterkamp 2005), so through this process, permafrost thaw also results in the transformation of forested areas into treeless, permafrost-free wetlands.

Considering that permafrost exerts a primary control on local hydrological processes (Woo 1986), permafrost disappearance has potentially profound implications to the flux and storage of water at local and basin scales. For

Received: 25 May 2012 / Accepted: 11 November 2012
Published online: 1 December 2012



Published in the theme issue "Hydrogeology of Cold Regions"

W. L. Quinton (✉) · J. L. Baltzer
Centre for Cold Regions and Water Science,
Wilfrid Laurier University, Waterloo, CanadaN2L 3C5
e-mail: wquinton@wlu.ca
Tel.: +1-519-8840710
Fax: +1-519-7251342

 DOI 10.1007/s10040-012-0935-2

example, permafrost limits the amount of infiltration to that which can be stored in the active (i.e. seasonally thawed) layer, and severely restricts hydrological interaction between near-surface supra-permafrost water and deep sub-permafrost groundwater. Permafrost also influences water storage and drainage patterns by physically supporting the active layer and by influencing its temperature, moisture, surface micro-topography, vegetation, snow cover and other factors (Jorgenson and Osterkamp 2005). Permafrost thaw is therefore transforming the surface and subsurface energy balance and ecology of the discontinuous permafrost region (Rawlins et al. 2009). There are also strong indications that permafrost thaw and disappearance are changing the region's hydrology. For example, the discharge from subarctic rivers in north-western Canada has increased in recent decades, particularly during low-flow periods (St. Jacques and Sauchyn 2009). However, the present ability to account for rising stream flows and capacity to predict flow variations is severely restricted by a limited understanding of the water flow and storage processes at the headwaters, and possible feedback processes during permafrost thaw that may influence them. This places considerable uncertainty about the future of water resources in the region.

In response to this uncertainty and the deficiencies of knowledge giving rise to it, the present study aims to increase the understanding of the fundamental properties and processes controlling the flow and storage of water in the headwaters of a wetland-dominated basin typical of the southern margin of the discontinuous permafrost zone. Specifically, the aim is to improve the understanding of the hydraulic response of peat plateaus and how it varies over a season as the active layer thaws, and over inter-annual periods as the permafrost beneath them thaws and disappears. For the latter, the permafrost thaw-induced ground surface subsidence, increased active layer thickness and reduced plateau surface area will be examined. Therefore the objectives of this paper are to examine (1) the thermo-physical properties of the active layer that control the hydraulic response of a peat plateau; and (2) how the permafrost thaw observed at the same plateau over the period 2001–2010 affects the (a) active layer properties and (b) subsurface runoff to an adjacent channel fen. Such an examination of fundamental properties and processes in the headwaters is a critical first step toward improving the capacity to predict the influence of ongoing permafrost thaw on the hydrology and water resources of the region.

## Study site and background

### Site description

Scotty Creek (61°18′ N, 121°18′ W) is a 152 km$^2$ drainage basin that lies 50 km south of Fort Simpson in the lower Liard River valley of the Northwest Territories, Canada (Fig. 1a), where the landscape is dominated by both discontinuous permafrost (Hegginbottom and Radburn 1992) and peatland complexes typical of the 'continental high boreal' wetland region (NWWG 1988). As such, Scotty Creek is also typical of the southern extent of permafrost where the large thermal offset created by dry, insulating peat preserves isolated patches of permafrost in the form of raised peat plateaus (Robinson and Moore 2000; Smith and Riseborough 2002). The Fort Simpson region has a dry continental climate with short, dry summers and long, cold winters. It has an average (1971–2000) annual air temperature of −3.2 °C, and receives 369 mm of precipitation annually, of which 46 % is snow (MSC 2011). Snowmelt usually commences in the second half of March and continues throughout most of April so that by May, only small amounts of snow remain (Hamlin et al. 1998). The Scotty Creek drainage basin is covered by 3–4 m of peat overlying a thick clay to silt-clay deposit of low permeability (Aylesworth and Kettles 2000).

### Hydrological function of major ground cover types

Remotely sensed data and ground observations at Scotty Creek indicate that several of the major peatland types along the southern boundary of permafrost have a specific hydrological function in the basin water balance. Peat plateaus have a limited capacity to store water, a relatively large snowmelt water supply and hydraulic gradients that direct excess water into adjacent permafrost-free wetlands (Wright et al. 2009). As such, the plateaus function primarily as runoff generators. Plateaus also obstruct and redirect water movement in adjacent wetlands since the open water surfaces of the latter occupy an elevation below the permafrost table. Bogs are primarily water storage features since they are surrounded by raised permafrost and therefore less able to exchange surface and near-surface flows with the basin drainage network. Unlike the bogs, channel fens conduct surface and near-surface flows along their broad, hydraulically rough channels; and, as such, an important function of these features is the lateral conveyance of water toward the basin outlet (Quinton et al. 2003).

### Permafrost thaw

Field monitoring of permafrost thaw at Scotty Creek began in 1999 with measurements along a ~40-m transect that traversed the southern tip of a ~0.08-km$^2$ peat plateau, between a channel fen on the west side of the plateau, and a flat bog on the east (Fig. 1b). Along this transect, thaw depth was measured at 1-m intervals by probing the ground with a graduated steel rod, which readily detected the top of the frozen, saturated peat (Wright et al. 2008). From these measurements, the width of permafrost was estimated as the distance between the points on either side of the plateau where permafrost was undetectable by the 1.3-m probe at the end of each summer thaw period (Quinton et al. 2011). Thaw of permafrost plateaus at Scotty Creek is driven by both vertical and horizontal energy flows. The vertical loss of permafrost is

 DOI 10.1007/s10040-012-0935-2

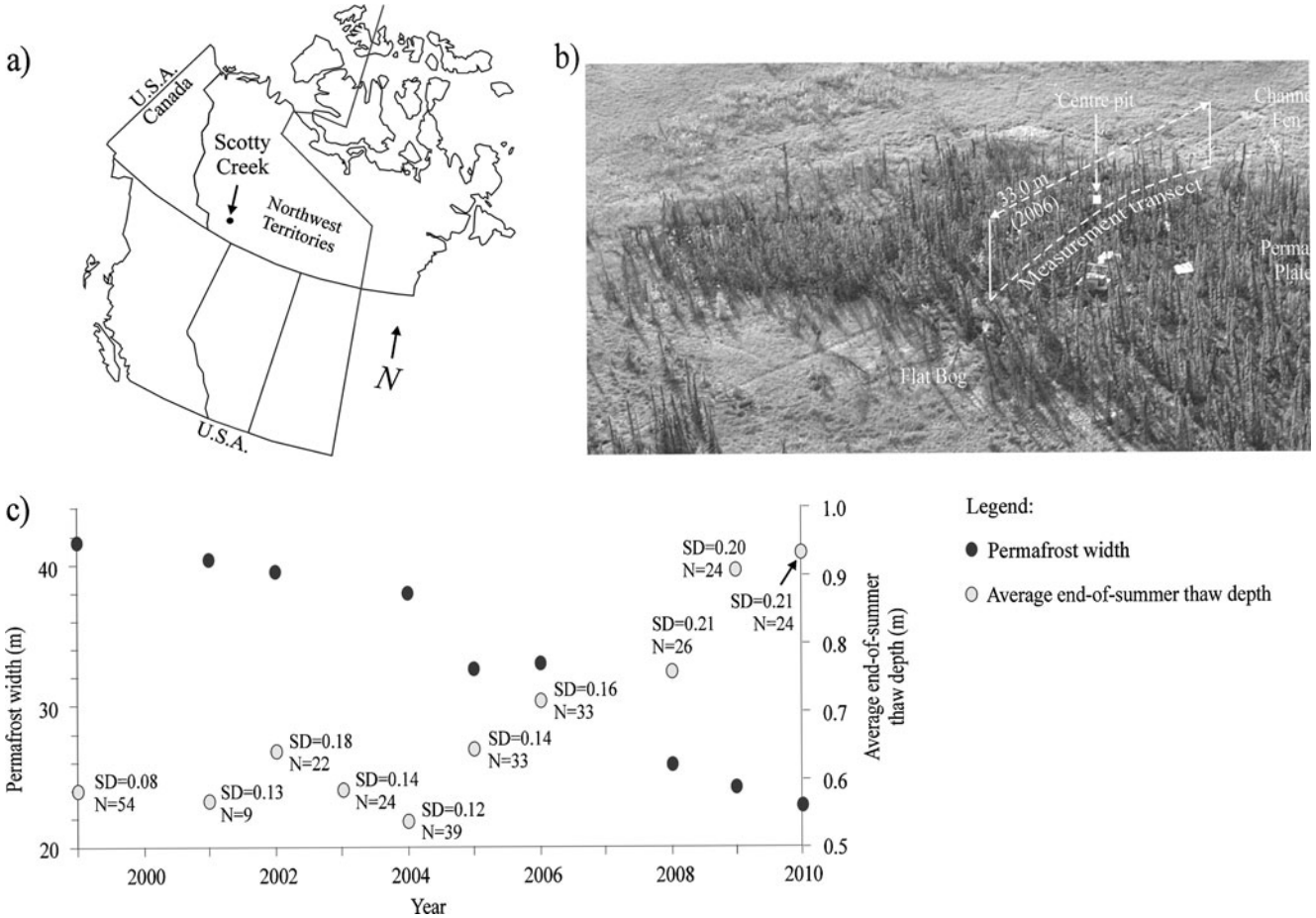


**Fig. 1** **a** The location of Scotty Creek within north-western Canada. **b** Oblique aerial photograph of the study plateau showing the location of the measurement transect and its width of 33.0 m measured in September 2006, when the photograph was taken. **c** Change in permafrost width and the average end-of-summer thaw depth for the period 1999–2010. *SD* is the standard deviation and *N* is the number of observations. Modified from Quinton et al. (2011)

proportional to active layer thickening. The average depth of thaw of the transect points by the end of summer (i.e. late August to early September) increased by approximately 0.36 m between 1999 and 2010, with the greatest increase in annual thaw depth occurring after 2004 (Fig. 1c). The vertical loss of permafrost since 1999 was therefore also ~0.36 m. For the same period, the horizontal energy flows from the adjacent bog and fen are indicated by changes to the permafrost width. The width of the permafrost body decreased from 41.6 m in June 1999 to 23.0 m by September 2010 (Fig. 1c). Permafrost thaw also led to subsidence of the plateau ground surface. For example, over the period 2006–2009, the ground-surface elevation of the transect points subsided on average by 0.13 cm—standard deviation (SD) = 0.12 cm; Quinton et al. 2011). Permafrost loss is not limited to this particular plateau but appears to be widespread throughout the Scotty Creek drainage basin. For example, the proportion of a 1-km$^2$ area of interest underlain by permafrost decreased from 70 to 43 % between 1947 and 2008 (Quinton et al. 2011). Given the contrasting hydrological functions of bogs, fens and plateaus, the permafrost thaw-induced transformation of one of these cover types into another, has direct consequences to local water flow and storage processes in the vicinity of thawing plateaus, and potential consequences to the basin hydrograph (Quinton et al. 2003).

## Active-layer properties

The soil profile of plateaus at Scotty Creek contain a relatively thin (~0.1–0.2 m) upper, lightly decomposed layer, overlying a darker layer in a more advanced state of decomposition. With increasing depth, the bulk density increases, while the porosity and average pore diameter decrease (Quinton and Hayashi 2007). Vertical profiles of saturated hydraulic conductivity ($K_S$) measured on peat plateaus exhibit uniformly high and uniformly low $K_S$ in the upper and lower regions of the soil profile respectively, separated by a transition zone in which $K_S$ decreases abruptly with depth (Quinton et al. 2008). The frost table is the thawing front and the boundary between the overlying thawed soil and underlying frozen soil. Although the exact position of the frost table in the soil profile is slightly different from the zero-degree isotherm due to a freezing-point depression (FPD), this isotherm serves as a good approximation of the frost table position (Carey and Woo 2000), owing to the relatively small

 DOI 10.1007/s10040-012-0935-2

magnitude of the FPD, and its depth-variation and variation from year to year. During soil thawing, the soil below the frost table is saturated or nearly saturated with ice and a small amount of liquid water. As such, the frost table is relatively impermeable to water, and represents the bottom of the subsurface flow zone—the thawed portion of the saturated soil that conducts lateral subsurface flow. Subsurface drainage from peat plateaus to adjacent bogs and fens, therefore, strongly depends on the depth of ground thaw. When the subsurface flow zone is near the ground surface, the flow rate is high, but as the soil thaws (i.e. frost table lowers), the depth of this zone increases and the subsurface flow rate therefore declines (Fig. 2).

Analysis of ~1-m-long soil cores from a peat plateau at Scotty Creek indicated substantial over-winter increases in volumetric soil moisture content, especially close to the ground surface (Quinton et al. 2008). For example, at 0.1 m depth, the moisture content increased from 0.3 (volumetric moisture content) at freeze-up in 2002 to near saturation (0.8) by late-winter, 2003. This suggests that over-winter moisture redistribution within the active layer can establish a near-saturated condition close to the ground surface prior to the melt of the overlying snowpack at the end of winter. Such a condition would limit the amount of snowmelt infiltration and promote rapid subsurface runoff from the plateau, since the meltwater would be restricted to the near-surface zone where the hydraulic conductivity is relatively high (Fig. 2). At the time that the snow cover disappears, the depth to the top of the saturated or near-saturated zone, is typically 10 cm as determined by the depth to refusal using the steel frost probe. For example, in late April and early May, 2011, the depth to refusal was measured at 26 evenly spaced points on the measurement transect (Fig. 1b) on the day that each became snow-free. The average depth to refusal was 10.9 cm, SD=6.5 cm, number of observations (N)=26. The relationship among the depth to refusal, the thawing front and the zero-degree isotherm at this initial time is unclear, as the 0–10 cm depth zone is typically unsaturated and may contain small ice fragments. Following this initial stage, the assumption is made that the depth to refusal indicates the thawing front depth and that the latter is approximated by the zero-degree isotherm (Hayashi et al. 2007).

## Evaporation and runoff

In 2004 and 2005, the evaporative flux was measured daily using five evaporation pans (for standing water) and 10 soil lysimeters (see Lafleur and Schreader 1994) placed throughout much of the ~0.005 km$^2$ area of the plateau shown in Fig. 1b (Wright et al. 2008). The total daily evapotranspiration (mm d$^{-1}$) from the plateau was computed as a weighted average based on the measured evaporation and percent cover of moss, lichen and pools on the plateau. For days when lysimeter data were

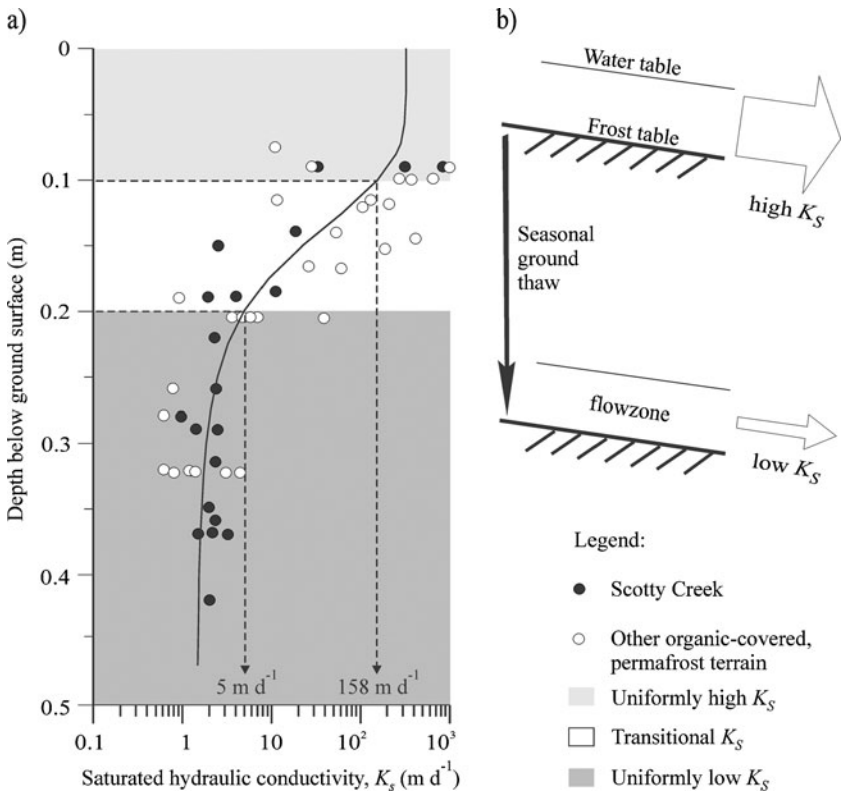


**Fig. 2** **a** Depth variation of saturated horizontal hydraulic conductivity measured from tracer ($KCl^-$) tests conducted at the site of the present study, as well as at other organic-covered permafrost terrains in north-western Canada, as reported by Quinton et al. (2008). The curve through the data is defined by Eq. 7. The *light and dark grey* indicate the zones in which $K_S$ is uniformly high and uniformly low, respectively. The schematic (**b**) indicates the decrease in the mean hydraulic conductivity of the saturated flowzone with active layer thaw. Modified from Quinton et al. (2008)

 DOI 10.1007/s10040-012-0935-2

unreliable due to rainfall, evapotranspiration (ET) from the plateau ground surface was estimated using the Priestley and Taylor (1972) method, with meteorological variables supplied by the meteorological tower and the ground heat flux computed from the thermocalimetric method described in Hayashi et al. (2007), using the temperature and moisture measurements at the Centre pit (Fig. 1b). The evaporative flux from the trees was not accounted for by Wright et al. (2008) and, as such, the ET estimate reported by Wright et al. (2008) was underestimated. However, the magnitude of the underestimate was thought to be relatively small owing to the much lower stand density than those studied in the southern boreal forest (e.g. Arain et al. 2003). The mean daily ET from the plateau weighted by the proportion of moss, lichen and pools was 1.4± 0.5 mm in the 2004 and 1.5±0.5 mm in the 2005 study period. The cumulative weighted ET was 56 mm ±8 mm by 4 June 2004; and 67 mm±6 mm by 8 June 2005 (Wright et al. 2008). The average value of the Priestley and Taylor $\alpha$ coefficient weighted by the relative proportion of the major cover types on the plateau, ranged from 0.68 to 0.91. Using the ET flux data provided by Wright et al. (2008), and raising the $\alpha$ value to 1.0 so that the flux increases to the equilibrium rate, runoff from the plateau would still exceed ET by at least a factor of 2.5.

Wright et al. (2008) also derived estimates of subsurface runoff from the plateau from the water balance using measurements at the Centre pit (Fig. 1b). To corroborate the water-balance-based runoff calculations, the authors estimated sub-surface runoff independently from the hydraulic gradient and conductivity using the Dupuit-Forchheimer approximation (Childs 1971). From the water-balance method, the total runoff was 238 mm ±71 mm by 4 June 2004; and 213 mm± 64 mm by 8 June 2005. For the same periods, the independent estimate indicated similar values: 175 mm in 2004 and 196 mm in 2005. The study by Wright et al. (2008) is important to the present study because it demonstrated that (1) the magnitude of ET is relatively small compared with runoff, i.e. $R$ was 3.1–4.3 times greater than ET in 2004, and 2.9–3.2 times greater in 2005; and (2) reasonable estimate of subsurface runoff from the plateau can be achieved from careful water-balance computations.

## Methodology

Direct runoff measurements were attempted numerous times at the study site using several designs of weirs and other flow conveyance structures, however in each case, the effects of icing led to flow breaches in the structure and consequently there was little confidence that these attempts produced reliable measurements of runoff for more than a just few days. This study therefore used the indirect methods of water-balance computation and model simulation to derive runoff. Both indirect methods required the subsurface and meteorological instrumentation and measurements described below.

### Subsurface measurements

The Centre pit (Fig. 1b) was excavated to the bottom of the thawed layer on 20 August 2001 so that soil sensors could be installed in profile. At the time of installation, the depth of thaw was 0.7 m, and the thermistors (Campbell Scientific, 107) were installed at 0.05, 0.1, 0.15, 0.2, 0.25, 0.3, 0.4, 0.5, 0.6, and 0.7 m depths. Water-content reflectometers (Campbell Scientific, CS615) were inserted horizontally at depths of 0.1, 0.2, 0.3, and 0.4 m. These sensors were calibrated using the water content of peat samples collected at the time of installation and measured gravimetrically (Quinton et al. 2005). A 92-cm$^3$ soil sample was taken next to each of the water-content meters at the time the sensors were installed in order to measure the soil porosity and bulk density following standard methods (Hoag and Price 1997). High-density PVC sample core tubes (inner diameter=0.15 m, length= 0.4 m) were inserted horizontally into the pit face at 0.09, 0.26, 0.29 and 0.37 m depths, in order to measure the variation in drainable porosity with depth. For each soil-sample core, the drainable porosity was measured as the ratio of the volume of water that freely drained from the sample to the volume of the soil sample (Quinton and Gray 2003). A PVC well with a 0.2-m inner diameter, was installed to the base of the thawed layer and equipped with a WL16 pressure transducer (Global Water) for monitoring the elevation of the water table. Following the installation of the sensors, the pit was backfilled with the excavated material, while preserving the original layering and groundcover as much as possible.

The study of Wright et al. (2008) evaluated how well the Centre pit represents the soil-moisture conditions of the plateau, by measuring the moisture content of the thawed portion of the active layer measured at 15 sampling points for 25 days in 2005 and comparing it with the moisture content of the Centre pit. The 15 points were located throughout the 0.005 km$^2$ portion of the study plateau shown in Fig. 1b. All measurements were within 1 m of the flagged point although their exact locations varied slightly to minimise disturbance, since the moisture content was measured gravimetrically by extracting 162-cm$^3$ soil samples at 0.05-m depth increments between the ground surface and the water table. The depth to the water table and frost table were also measured daily at each sampling point, with a ruler and graduated steel rod. The daily standard deviation of the total unfrozen moisture depth measured below each of the 15 sampling points varied between 31 and 96 mm, indicating a relatively high spatial variation of moisture storage on the plateau. Wright et al. (2008) compared the sum of the average total change in liquid water content of the 15 points for the 25 measurement days (47 mm) with the total change in liquid water content at the Centre pit for the same 25 days (44 mm) and concluded that the soil moisture content measured at the Centre pit represents the

 DOI 10.1007/s10040-012-0935-2

average moisture conditions of the overall plateau reasonably well.

### Meteorological measurements

Air temperature was measured near the Centre pit in 2003 and at a meteorological station located between the two pits in 2004 and 2005 using a thermistor housed in a Gill radiation shield. Air temperature was measured using a Campbell Scientific 107B thermistor in a Gill shield, and ground-surface temperature was measured using an infrared thermocouple (IRT) sensor (Apogee Instruments, IRTS-P) located at a height of 1.5-m above the ground. Snow depth was measured with a Campbell Scientific SR50 sonic sensor. The above measurements were made near the Centre pit prior to August 2003. Since then, measurements have been made from a meteorological station located roughly mid-way between the two pits. All sensors were connected to dataloggers (Campbell Scientific, CR10X), programmed to measure every minute and record half-hourly averaged values. A tipping-bucket rain gauge (0.2 m diameter, 0.35 m height) calibrated to 0.25 mm per tip was used to obtain a continuous record of rainfall input to the plateau ground surface. All sensors were connected to Campbell Scientific CR10X dataloggers, programmed to measure every minute and averaged and recorded every 30 min.

### Water-balance computation of plateau runoff

Annual water balances were computed for each year for the period 1 September to 1 September, beginning in 2001, with the exception of 2009 when equipment failure resulted in loss of data needed for the computations. The present study used the same methods of field measurement and computation used by Wright et al. (2008) for shorter periods in 2004 and 2005. In the present study however, runoff was derived from the water balance for two periods in each year, one ending 1 June, which is dominated by the freshet, and the other ending 1 September, which includes the influence of summer rain events. For both periods, computations of runoff began on the first day of snowmelt at the end of winter. The final year of computation ended 1 September 2010. Using measurements at the instrumented soil pit, the change in depth of unfrozen moisture in the active layer was computed from:

$$\Delta W = (R_i + P + M_S + I_M) - (R_o + \mathrm{ET} + I_F) \quad (1)$$

where $R_\mathrm{i}$ is subsurface runoff to the pit, and $P$, $M_\mathrm{S}$ and $I_\mathrm{M}$ are the daily total contributions of water from rainfall, snowmelt and melt of ice in the active layer respectively. $R_\mathrm{o}$ is the subsurface runoff from the pit, and ET and $I_\mathrm{F}$ are the daily losses to evapotranspiration and freezing of water in the active layer. All terms have units of mm. A positive $\Delta W$ implies a gain in water storage, while a negative value implies a loss. Equation (1) was rearranged to solve for $R_\mathrm{o}$ and thereby obtain estimates of subsurface runoff from the peat plateau for daily and seasonal periods. $I_\mathrm{F}$ was assumed to be zero during soil thawing, and $R_\mathrm{i}$ was assumed to be negligible given the location of the pit near the crest of the plateau. With the exception of ET, the remaining terms were computed on 30-min intervals, and then summed to arrive at daily and seasonal totals. Neither the water-balance computations nor the model simulations derived ET independently, and as a result, the ET flux is included in both the computed and simulated runoff. However, given that runoff is much larger than ET at the study site (Wright et al. 2008), it is thought that the runoff estimates in this study are still useful for examining possible impacts of permafrost thaw on plateau runoff.

Based on the spacing of the water-content meters, four depth ranges were defined: 0 to <0.15, 0.15 to <0.25, 0.25 to <0.35, and 0.35–0.70 m. The profile water content, W, was obtained from the sum of the unfrozen moisture depths of the four computational layers:

$$W = W_{\mathrm{L}(1)} + W_{\mathrm{L}(2)} + W_{\mathrm{L}(3)} + W_{\mathrm{L}(4)}. \quad (2)$$

During soil thawing, the boundary between the frozen and unfrozen peat can be approximated by the zero-degree isotherm, i.e. the frost table (Woo 1986). The time when the frost table reached the depth of each soil thermistor was recorded, and used to produce a continuous, half-hourly record of frost table depth by interpolation. As the frost table descended sequentially through each computational layer, its position was used to partition the layer containing the frost table into the thawed zone above the frost table, and the frozen zone below it, from:

$$f_\mathrm{th} = (\mathrm{FT_{int}} - L_\mathrm{d})/L_\mathrm{th}, \quad (3)$$

where $\mathrm{FT_{int}}$ is the frost table depth of each 30-min interval, $L_\mathrm{d}$ is the depth of the top of the computational layer below the ground surface, and $L_\mathrm{th}$ is the thickness of the computational layer. The depth of water above and below the frost table, in the layer containing the frost table, was computed from Eqs. (4) and (5) respectively:

$$W_\mathrm{La} = f_\mathrm{th} \times L_\mathrm{th} \times \mathrm{VWC_{int}}, \quad (4)$$

$$W_\mathrm{Lb} = (1 - f_\mathrm{th}) \times L_\mathrm{th} \times \mathrm{VWC_{PT}} \quad (5)$$

where $\mathrm{VWC_{int}}$ is the volumetric water content measured in each interval, and $\mathrm{VWC_{PT}}$ is the volumetric water content of the layer just prior to thaw. $W_\mathrm{L}$ for the layer containing the frost table was then computed from the sum of $W_\mathrm{La}$ and $W_\mathrm{Lb}$. For layers entirely below the frost table, $W_L = L_{th} \times VWC_{PT}$, and for layers entirely above the frost table, $W_L = L_{th} \times VWC_{int}$.

Estimating the amount of water released per unit increase in frost table depth requires knowledge of the water-equivalent depth of ice in the active layer prior to the onset of thaw. The latter was estimated from the average total (ice + water) moisture content of the two

 DOI 10.1007/s10040-012-0935-2

frozen soil cores sampled from near the Centre pit. Although these samples of April 2003 were the only ones taken over the multi-year study period, compared with the other years, they represented an average late-winter condition in terms of ice content based on the active layer moisture content at the end of the previous summer (Wright et al. 2009; Fig. 6). The water-equivalent depth of ice released into the active layer per 30-min interval was computed from:

$$I_{M(int)} = (VWC_{int} - 0.2) \times \Delta FT \times 0.9, \quad (6)$$

where 0.2 represents the average water content of the computational layers during winter, ΔFT is the change in frost table depth between successive 30-min intervals, and 0.9 accounts for the difference in volume of ice and water. The daily contribution of water from the melt of ice in the active layer $I_M$ was computed from the sum of the difference between consecutive, 30-min computations of $I_{M(int)}$.

### Model simulation of plateau runoff

Subsurface runoff from the study plateau was simulated using the cold regions hydrological model (CRHM) platform, a flexible object-oriented modelling system devised for purposes of simulating the cold regions hydrological cycle from hillslopes to medium-sized basins. CRHM has no provision for calibration; parameters and model structure are selected based on the understanding of the hydrological system. As such, the model can be used both for prediction and for diagnosis of the adequacy of hydrological understanding. A full description of the CRHM platform is provided in Pomeroy et al. (2007).

CRHM requires that the slope gradient, the overall active layer thickness, the initial position of the top of the frozen, saturated layer—approximated by the thawing front (Quinton and Hayashi 2007)—the initial water equivalent of the snowpack, and the number of computational soil layers be defined. For each soil layer, key thermal (i.e. volumetric heat capacity) and physical (i.e. bulk density and porosity) properties, and initial soil temperature must be defined. Within each layer, the depth of water (m) held by surface tension may be set as a constant value, or may be calculated from the van Genuchten (1980) expression. Any excess water is assumed to be available for subsurface drainage.

The initial snow-water equivalent (SWE) for the snowpack in each year must be defined for each CRHM run. The model computes the SWE depletion using the temperature-index approach (Dingman 2002, p. 210), which is based on the association between cumulative air temperature and snow melt. CRHM requires that an offset in temperature and a coefficient be supplied by the user. For this study, these values were determined by trial and error until the computed SWE depletion matched the observed depletion. CRHM uses an analogous method of computing the ground thaw rate, although cumulative ground surface temperature is used instead of the cumulative air temperature. As for SWE depletion, an offset and coefficient must be specified. In the present study, their values were derived by trial and error until the match between the measured (Fig. 6c) and computed thaw was optimised. Although these temperature index methods used to simulate snowmelt and frost table lowering are relatively simple, their use has several advantages, since (1) the present study is focussed on improving the understanding of subsurface runoff processes, and (2) index methods enable a close match between the measured and simulated snowmelt and frost table lowering, and therefore removes the possibility that significant error in the runoff simulations results from the snowmelt and ground thaw routines.

Running the model required air temperature, ground surface temperature and rainfall, all of which were measured at 30-min intervals on the study plateau. All computations were made on a 30-min time step for a 1-m wide strip of ground extending ~20 m (depending on the year) from the crest of the plateau to its edge with the adjacent channel fen. The upper boundary of the strip was the ground surface, and its lower boundary was the impermeable frost table. In August 2002, the plateau was 39.5 m wide and the modelling strip was taken to be half this length (i.e. 19.8 m), the approximate distance from the plateau crest to its edge. A constant hydraulic gradient of 0.019 was used, equal to the average hydraulic gradient measured between the crest and the edge of the plateau on 30-min intervals over the June–August period in 1999. These measurements preceded the installation of the Centre pit, but their location coincided with the modelling strip used in this study. The same four computational layer soils layers used for the water-balance calculations were also used in CRHM.

To capture in a continuous function the high hydraulic conductivity near the ground surface, its large reduction in the transition zone, and its low, asymptotic value in the bottom zone (Fig. 2), the following equation was proposed:

$$\log K_S(z) = \log K_{S\,btm} + \left(\log K_{S\,top} - \log K_{S\,btm}\right)/[1 + (z/z_{trn})^n] \quad (7)$$

where $z$ [L] is depth below the ground surface, $K_{S\ top}$ and $K_{S\ btm}$ are the hydraulic conductivity [$LT^{-1}$] of the top and the bottom of the peat profile, $z_{trn}$ [L] is the transition depth, and $n$ is a dimensionless constant governing the shape of the transition curve (Quinton et al. 2008). The simulations used the default values of $K_{S\ top}$=360 m $d^{-1}$, $K_{S\ btm}$=1.4 m $d^{-1}$, $z_{trn}$=0.15 m and $n$=4.3, as defined by Quinton et al. (2008) for organic soils from Scotty Creek and other similar sites.

As with the water-balance computations, CRHM was run for two periods in each year for the period 2002–2010 (except 2009)—one ending 1 June which is dominated by the freshet, and the other ending 1 September, which includes the influence of summer rain events. For both

 DOI 10.1007/s10040-012-0935-2

periods, the runoff simulations began on the first day of snowmelt at the end of winter. For each year, CRHM was run three times for both time periods. The initial simulations for each year assumed that the maximum end-of-summer thaw depth was 0.7 m, the end-of-summer thaw depth measured in August 2001 when the Centre pit was excavated. They also assumed a constant modelling strip length and hydraulic gradient equal to that measured in 2002, when the first simulations were made. These runs therefore simulated the plateau runoff assuming there was no permafrost thaw over the 2001–2010 period of simulations. In order to quantify the effect of thaw and subsidence on plateau drainage, the simulations were re-run according to three conditions. Re-run A represented the year-to-year reduction of the hydraulic gradient resulting from permafrost-thaw induced subsidence of the plateau ground surface. Re-run B included changes to the hydraulic gradient represented in the latter, plus the observed year-to-year increase of the annual thaw depth. Finally, re-run C included the changes in hydraulic gradient and thaw depth represented by B, plus the observed decrease in plateau surface area. Since the water flow simulations were made for a 1-m wide strip extending from the middle of the plateau to the edge of the fen, only the year-to-year change in the length of this strip had to be specified in order to represent the change in the runoff producing area.

## Results and discussion

### Active-layer properties

#### Seasonal liquid moisture dynamics

The subsurface runoff rate from a peat plateau depends upon the depth of the impermeable frost table, and the thickness of the thawed, saturated zone that conveys subsurface runoff from the plateau. That is, the subsurface runoff rate depends upon the ice and water content of the active layer. Over the course of a year, the amounts of water and ice in the active layer vary due to (1) melt or freezing of in situ moisture, and (2) moisture gains to and losses from the active layer. Figure 3a depicts the annual thawing and freezing cycle in the Centre pit at 0.3 m depth for 2003–2004 with no change in the total moisture content, except for the 9 August–1 September period when the volumetric soil moisture fell below saturation.

The FPD was defined as the minimum temperature to occur during the zero-curtain period. The duration of the latter was measured as the number of consecutive days that the average daily temperature at the depth of interest did not change by more than 0.1 °C. In 2003, the zero curtain period at 0.3 m depth extended for the 41 days between 4 November and 14 December (Fig. 4b), during which time the liquid volumetric moisture content decreased from 0.7 to 0.43. The FPD of this period was −0.4 °C, comparable to the average FPD for the 2001–2010 study period of −0.3 °C, SD=0.1, $N$=8. Toward the end of the zero-curtain period (7 December), the rate of reduction in the liquid moisture fraction increased as indicated by the increased spacing between the daily data points (Fig. 3a), which corresponds to the change in slope of the time series of liquid moisture content for 0.3 m depth shown in Fig. 4c.

Between the minimum average daily temperature of −6.2 °C and the FPD temperature of ca. −0.3 °C, the unfrozen moisture content remained near 0.2 (Fig. 4c), the winter period unfrozen moisture content shown in Fig. 3a. Laboratory measurements on samples taken from the Centre pit (Quinton and Hayashi 2007) indicate that 0.2 is the residual moisture value for tension heads greater than ca. 5 m. Ice in the soil began to melt once the temperature rose above ca. −0.3 °C, and continued warming returned the soil to the thawed, saturated state it was in when it froze the previous autumn (Fig. 3a). The freezing process followed a similar pattern, whereby moisture remained in the frozen state until the FPD temperature was reached. During soil freezing, most of the decrease in water content occurred in the narrow range between −0.3 and −0.7 °C, as further cooling below −0.7 °C had little effect on the water content.

The peat at 0.3 m depth was saturated when it froze in the autumn of 2003 (Fig. 3a). In other years, the peat at this depth was unsaturated when freezing; for example, the unsaturated period of 9 August to 1 September 2004 (Fig. 3a) persisted until the peat froze in the autumn of that year (Fig. 3b). When the soil thawed in the following spring (2005), the volumetric soil moisture had risen by 0.1 and returned to saturation. Although no direct measurements of moisture migration were made over the winter, the overlying snowpack can be ruled out as the source of water since no significant over-winter melt events occurred in that year. Likewise, lateral seepage is unlikely given the position of the Centre pit on the crest of the plateau. This leaves vertical moisture migration from lower depths in response to the gradients of temperature and vapour pressure as the most likely source. The increase in moisture content between freeze-up and thaw was greatest at the 0.1-m measurement depth, where, for over the 2001–2010 period, the average moisture content at freeze-up (e.g. the moisture content at which the freezing limb intersects the zero-degree line in Fig. 3) was 0.41 ($\sigma$=0.08), but increased to 0.76 ($\sigma$=0.01) at the time of thaw. The latter is taken from the stable moisture content reached generally within 4 or 5 days after the thawing limb crosses the zero-degree line. The difference between these values suggests an average over-winter increase in moisture of 0.34 per volume ($\sigma$=0.09).

Comparison of Fig. 3a and b indicates some obvious differences between these two consecutive years. For example, the minimum temperature during the 2004–2005 annual period of −2.4 °C was approximately 4° warmer than in the preceding winter, and the zero curtain (24 October–16 November) was 24 days in length and considerably shorter than in the previous year. These differences do not appear to have resulted from differences in air temperature or snow depth. For example, the average daily temperature for the 1 November to 31

 DOI 10.1007/s10040-012-0935-2

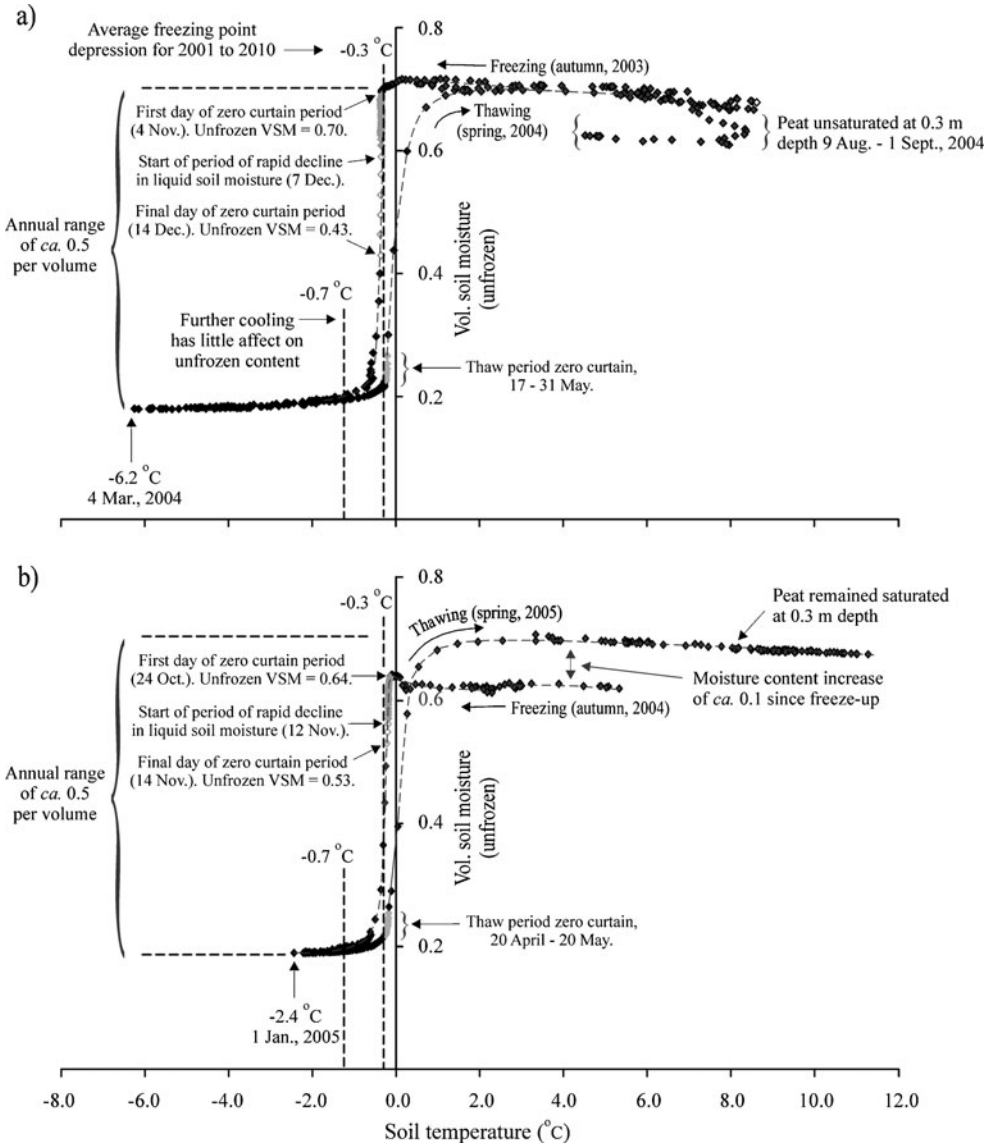


**Fig. 3** The unfrozen volumetric moisture content and soil temperature measured at 0.3 m depth in the Centre pit for a 1-year period commencing **a** 1 September 2003 and **b** 1 September 2004. *Grey symbols* indicate the zero-curtain period

March period differed by only 0.1 °C between the two winters. In 2003, the snow pack formed a bit later (23 October) than in 2004 (16 October). Although the daily average snow depth from the time of formation until 30 November was 21 cm in 2003 and only 6 cm in 2004, from the beginning of December onward the snowpack depth of the 2 years was very similar.

A wetter autumn period in 2003 appears mainly to have affected the onset date and duration of the zero-curtain period (ZCP). The total August and September rainfall in 2003 was 120 mm but only 32 mm in 2004. As a result the, freeze-up period in 2003 was relatively wet. The average unfrozen moisture content in the Centre pit (e.g. Fig. 4d), for period 1 September to 31 October, was 420 mm in 2003 but only 368 mm in 2004. Therefore, an extra 52 mm of moisture had to freeze in 2003–2004. This would account for the later occurrence of the onset of the zero-curtain in 2003 as more time would have been needed to lower the soil temperature to the FPD. The wetter conditions of 2003 would also account for the longer duration of the zero curtain period, since a greater amount of water had to be converted to ice before further cooling (i.e. below the FPD) could resume. The wetter active layer during the freezing period of 2003 also meant that the active layer in that year was more thermally conductive and therefore better able to lose heat content to the atmosphere. This may account for the lower annual minimum temperature of the Fig. 3a. The later occurrence of this temperature in Fig. 3a (4 March) than in Fig. 3b (1 January) may indicate that the active layer continues to cool for a longer period when in a relatively wet condition.

The ca. 7-month snow-covered period in each year (e.g. Fig. 4a) coincided with the period when soil temperatures were at or below the FPD temperature (Fig. 4b). In 2003, for example, ground temperatures at

 DOI 10.1007/s10040-012-0935-2

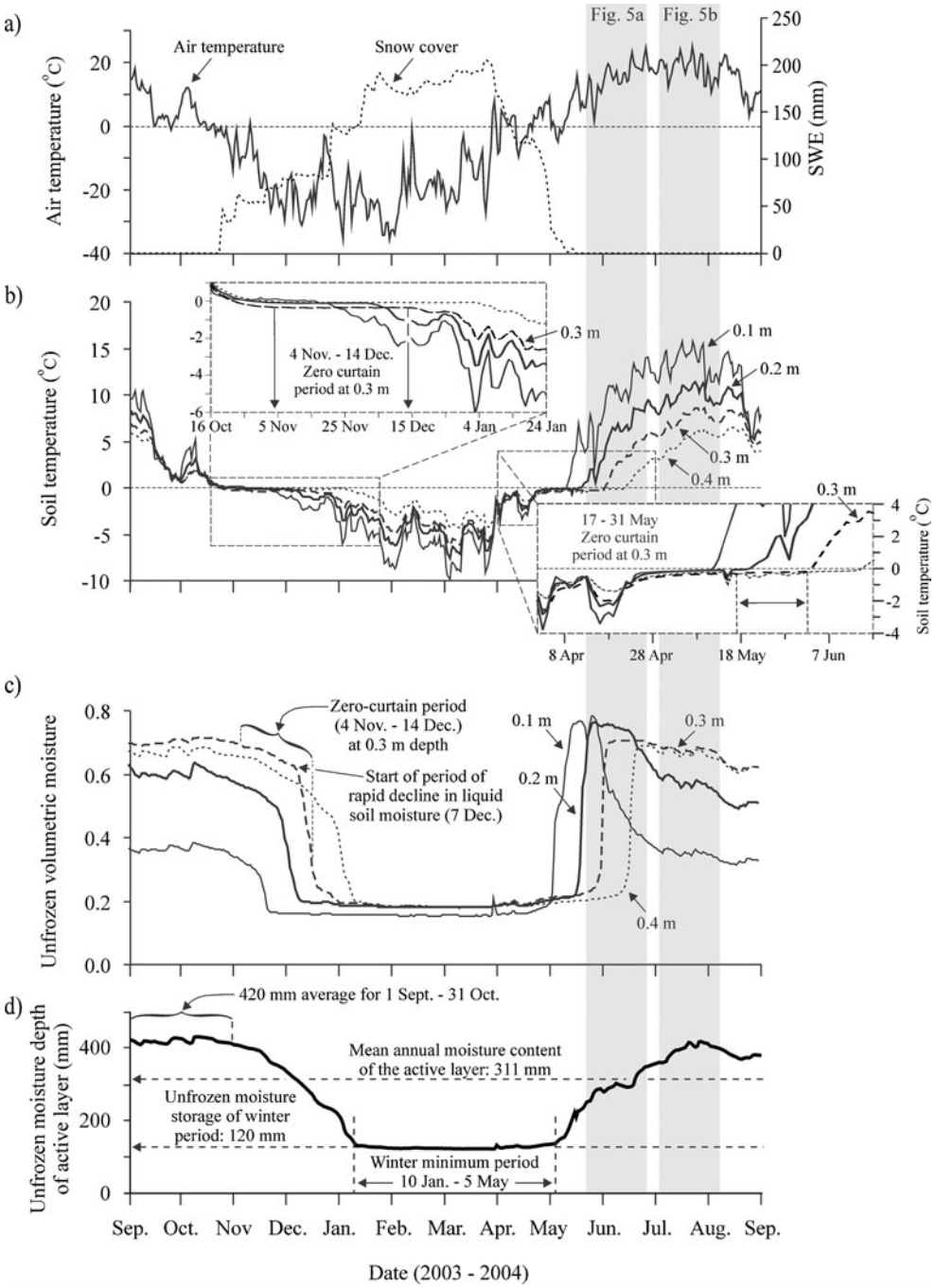


**Fig. 4** Measurements from the meteorological station and Centre pit for the annual period beginning 1 September 2003. **a** Air temperature and snow-water equivalent (SWE); **b** Soil temperatures from four selected depths; **c** Unfrozen volumetric moisture content at the same four depths; and **d** Unfrozen moisture content of the active layer computed from Eq. 2, assuming an active layer thickness of 0.7 m as measured in August 2001 when the Centre pit was installed

the four depths plotted in Fig. 4b reached the FPD between 22 October and 16 November. The duration of the zero curtain period that followed increased with depth. For the six measurement depths between 0.05 and 0.3 m, the zero curtain duration ranged from 20 to 47 days. The duration increased to between 63 and 90 days for the four measurement depths between 0.4 and 0.7 m. The increasing duration of the zero-curtain with increasing depth reflected the greater moisture contents at depth where more latent energy was released to complete the freezing process. For example, based on the difference in unfrozen moisture content before and after freezing at each depth, the latent energy released was about 3.6 times greater at 0.3 m than at 0.1 m for 2003–2004. Regardless of the moisture content prior to freezing, it decreased to approximately 0.2 per volume as the soil temperature lowered to −0.7 °C (Fig. 4c).

 DOI 10.1007/s10040-012-0935-2

The duration of the zero curtain period also increased with depth during soil thawing, but the durations were often shorter. In 2004, the durations increased from 8 days at 0.05 m to 65 days at 0.7 m (e.g. Fig. 4b). The zero curtain duration during thawing at 0.3 m depth was 15 days (17–31 May) in 2004 (Fig. 3a) and 30 days (20 April to 20 May) in 2005 (Fig. 3b).Thermal ripening and melt of the 0.8 m deep (205-mm SWE) snowpack above the Centre pit began on 28 March 2004 when the air temperature rose above 0 °C (Fig. 4a). Although the Centre pit remained snow-covered until 15 May, the temperature at 0.1 m rose above the freezing point depression on 11 May, and the unfrozen moisture content at this depth rose sharply on 1 May. The slightly earlier rise in the moisture content than the thaw at 0.1 m, suggests that this depth may have been affected by water input from an external source, namely meltwater from the overlying snowpack. For the measurement depths below 0.1 m, the rise in unfrozen moisture content (Fig. 4c) coincided with the rise in the temperature above the FPD (Fig. 4b).

The computation of the total unfrozen moisture stored in the 0.7-m profile indicated that over the course of the year, there were two distinct levels of unfrozen moisture. A winter level characterised the 4-month winter minimum period (e.g. approximately 10 January to 5 May in 2004) when soil temperatures were below −0.7 °C throughout the profile, and where the unfrozen moisture content remained close to 120 mm (Fig. 4d). During summer, the depth of unfrozen moisture in the profile ranged between 370 and 430 mm. The transition between these two storage levels was smoothed by the sequential freezing and thawing of successive depths depicted in Fig. 4c. The analysis of temperature and moisture variations at the Centre pit for the other years of this study produced similar results.

### *Hydraulic response to rainfall*

Given that both the horizontal saturated hydraulic conductivity ($K_S$) and drainable porosity vary with depth (Quinton et al. 2008), the hydraulic response of a peat plateau depends upon the vertical position of the thawed, saturated zone at the time that it receives snowmelt or rainfall input. This saturated zone, bounded by the water table and frost table on its upper and lower edges respectively, descends through the peat profile as the ground thaws. Figure 5a shows a typical hydraulic response observed early in the thaw season, shortly after snow cover removal in 2004 (Fig. 4a), while the upper 0.4 m of active layer was still thawing (Fig. 4b) and draining (Fig. 4c). The 34-mm event of 25–27 May commenced with the water table at a depth of ~0.05 m. At that depth, the drainable porosity measured in the laboratory was 50 % (Quinton and Hayashi 2007) and, therefore, the water-table rise to above the ground surface (as indicated by an apparent change in slope in the water level record) was expected (Fig. 5a). The subsequent 12.5 mm that fell onto the ponded water on 27 May produced an approximately equivalent rise in the water table. Figure 5a depicts a condition of high subsurface runoff as the saturated zone was within the zone of uniformly high $K_S$ (Fig. 2) for an extended period.

Despite the relatively deep frost table in late summer, a water-table rise can be rapid due to the high rate of percolation through the unsaturated peat to the zone of high-water content above the water table. The water-table rise can also be large, due to the relatively low drainable porosity at depth. For example, prior to the relatively small (9.3 mm) rainfall of 19 July 2004, the water table was 0.45 m below the ground surface and the frost table had already reached the bottom of the Centre pit at 0.7 m (Fig. 5b). During this 2-h event, the water table rose by 0.16 m, indicating a field-based drainable porosity of 6 %, which is consistent with the drainable porosity measured in the laboratory (Quinton and Hayashi 2007) on soils sampled from 0.4 to 0.5 m below the ground surface.

Despite the relatively large water-table rises shown in Fig. 5b, they were insufficient to displace the saturated zone above the zone of uniformly low $K_S$. However, the drainable porosities at these depths are sufficiently low that larger rain events may cause the water table to rise from an initially deep position into the zone of uniformly high $K_S$, enabling a large hydraulic response. For example, in 2010, the 26.8-mm rainfall of 15 July produced a water-table rise of 18.7 cm from an initial depth of 27.1 cm (Fig. 5c). The magnitude of that rise is consistent with the drainable porosity of 15 % measured in the laboratory (Quinton and Hayashi 2007) for samples from ~0.27 m depth. Such storm events produce rapid runoff from the plateau by displacing the saturated layer into the zone of uniformly high $K_S$, where $K_S$ is two orders of magnitude higher (Quinton et al. 2008). An additional 14 mm rainfall on 16 July prolonged the water table in this highly conductive peat layer (Fig. 5c).

### *Active-layer change*

The permafrost thaw and ground subsidence measured on the study transect (Fig. 1c) was accompanied by changes to the active layer measured at the Centre pit, where the data indicate that active layer moisture (Fig. 6a) and temperature (Fig. 6b) steadily rose since monitoring began in August 2001. The greatest increase in moisture was at 0.1 m where with the exception of 2007–2008, the average value increased with each successive year from a minimum of 0.26 in 2001–2002 to a maximum of 0.36 in 2009–2010. This is an important observation since wetter conditions near the ground surface allows for a more efficient conduction of thermal energy from ground surface into the active layer. The range in moisture content at 0.1 m between freeze-up and thaw decreased in each successive year (except 2004–2005) from 0.45 in 2001–2002 and 0.22 in 2009–2010. Over these years, the moisture content that the 0.1 m depth adjusted to within a few days after it thawed varied over a narrow range of values close or equal to saturation: 0.74 (2007) to 0.77 (2002 and 2003), with no apparent increase or decrease

 DOI 10.1007/s10040-012-0935-2

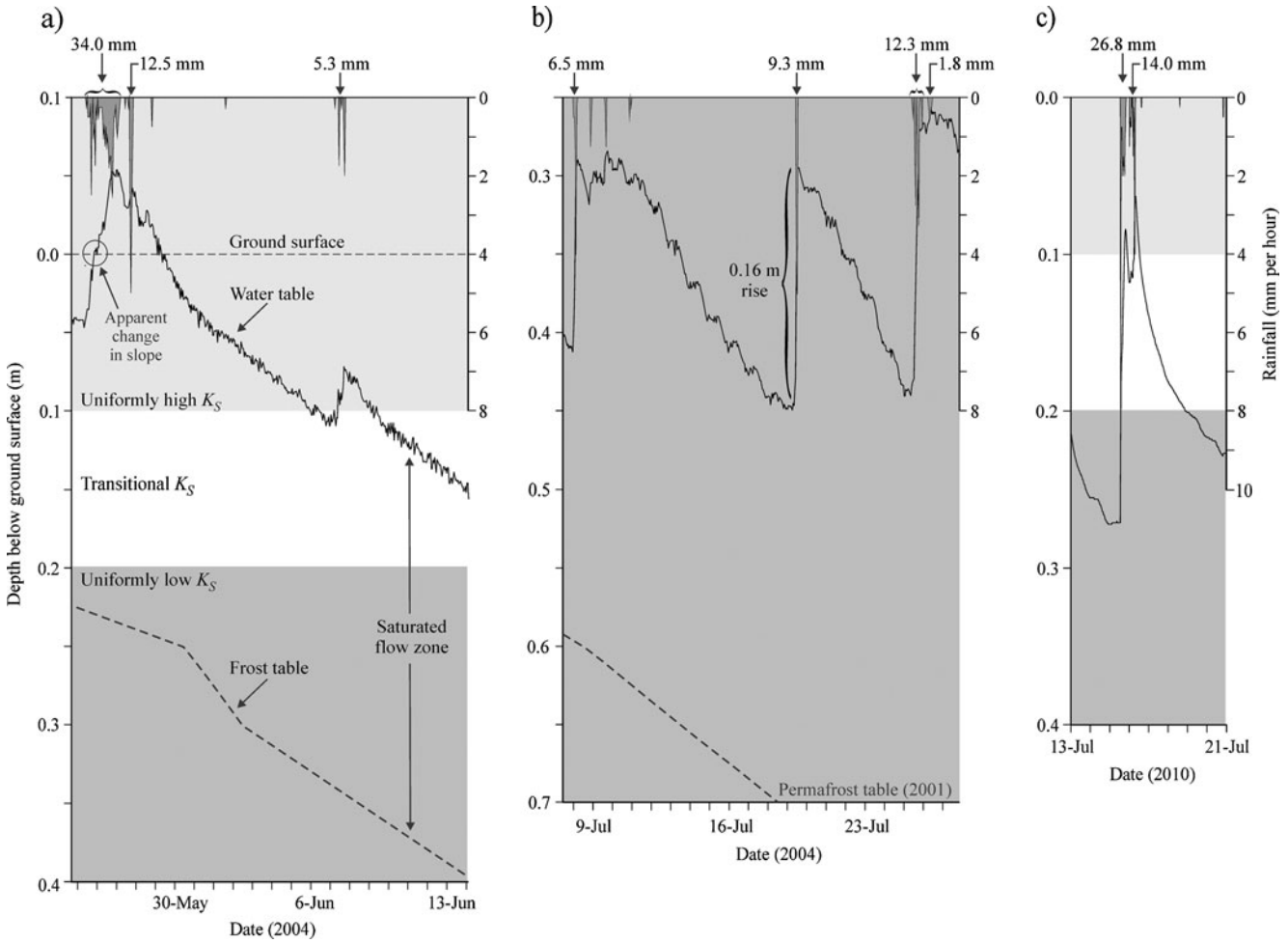


**Fig. 5** Water table response at the Centre pit to selected rainfall events in **a** the early summer of 2004 and the late summer of **b** 2004 and **c** 2010

from year to year. However, with the exception of 2005, the moisture content at 0.1 m at freeze-up (i.e. the moisture content that intersects the zero-degree vertical line in Fig. 3b) increased with each year from 2001 (0.32) to 2010 (0.54). Also, the maximum annual temperature at the deepest sensor (0.7 m) increased with each successive year between 2001 (2.0 °C) and 2009 (8.1 °C), followed by a slight decrease in 2010 (7.5 °C). The soil temperatures also indicate that active layer thaw occurred earlier in the year as the decade progressed. For example, each of the four depths shown in Fig. 4b thawed about 20 days earlier near the end of the study (e.g. 2010) than near the beginning (e.g. 2002).

As the active layer at the Centre pit (i.e. 0–0.7 m) warmed over the decade, its liquid-moisture content increased. For example, the mean annual liquid-moisture content of the Centre pit increased from 311 mm in 2003–2004 (Fig. 4d) to 376 mm by 2009–2010 (Fig. 6a). Likewise, the number of days per year that any depth in the active layer was thawed and, therefore, able to conduct subsurface flow increased throughout the decade—for example, the 0.3 m depth position discussed in relation to Fig. 3 was thawed and therefore able to conduct water for 141 days in 2003–2004 (Fig. 3a) and 144 days in 20042005 (Fig. 3b). Over the study period, the number of days that this depth was thawed and able to conduct runoff increased from 127 in 2001–2002 to 163 by 2009–2010.

To investigate this further, thaw curves were plotted for each year based on the date when the average daily temperature at each of the 11 thermistor depths in the Centre pit changed sign from negative to positive (Fig. 6c). Some degree of shift to earlier thaw dates was noted as the decade progressed. For example, after the first 3 years of study (2002–2004), the date when active layer thaw reached 0.7 m appears to have shifted to approximately 15 days earlier. The dates of thaw initiation also generally shifted to the left (i.e. earlier) as the decade progressed. Over the course of each thaw season, the thermal gradient driving the thaw process decreases as the distance between the ground surface and the thawing front below increases. Despite this, the thaw curves presented in Fig. 6c appear remarkably unattenuated compared with thaw curves derived by the authors in other study locations by the same method (e.g. Quinton et al. 2000, 2005). Hayashi et al. (2007) rigorously tested the thermal data from the Centre pit by computing the ground heat flux from the calorimetric, gradient, and flux-plate

 DOI 10.1007/s10040-012-0935-2

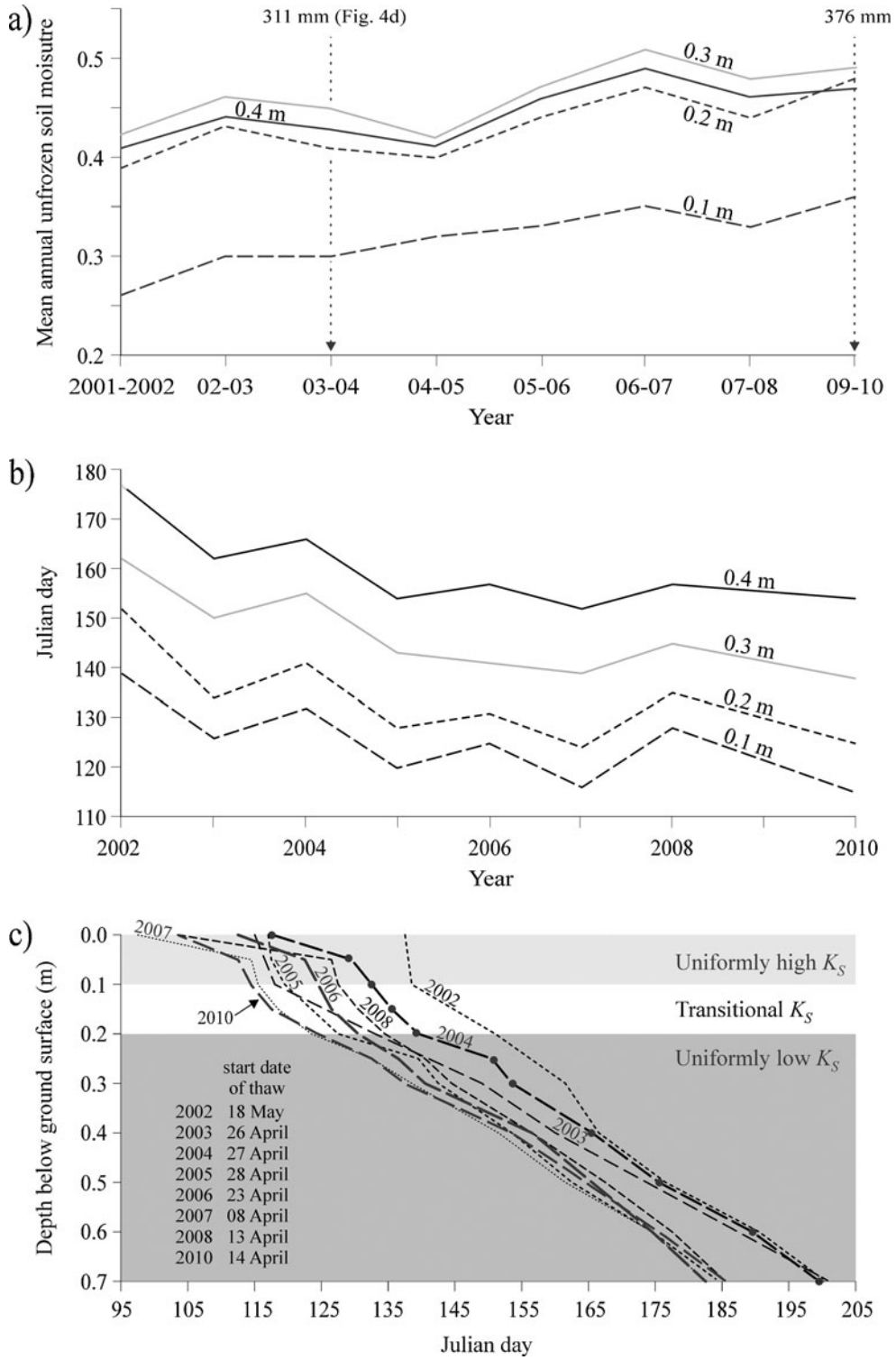


**Fig. 6** **a** Mean annual unfrozen soil moisture content at *0.1*, *0.2*, *0.3* and *0.4* m depths in the Centre pit for each annual period beginning with 1 September 2001 and ending with 1 September 2010. The mean unfrozen moisture depth of the active layer of *311 mm* for the year 2003–2004 is identified for comparison with Fig. 4d. **b** The date that the *0.1*, *0.2*, *0.3* and *0.4* m depths rose above 0 °C in each year of the study, starting with the spring thaw of 2002. **c** Soil thaw curves for each year of study. The curves were defined by interpolation between points representing the date when the average daily temperature at each measurement depth at the Centre pit rose above 0 °C. These dates are identified with *black dots* for 2004. The initial thaw date for each year is also provided (*lower left*)

methods, all of which compared closely, increasing the confidence in the data set. The reasons for the apparent lack of attenuation in the thaw curves are therefore unclear and require further investigation.

 DOI 10.1007/s10040-012-0935-2

## Active-layer runoff

The preceding discussion on the thermo-physical properties of the active layer, their control on the hydraulic response of a peat plateau, and how the active layer is changing with permafrost thaw provides the wherewithal for the following examination of how the subsurface runoff from a peat plateau is affected by on-going permafrost thaw.

### Water-balance computations and simulation

The estimates of plateau runoff from the model simulations and water-balance computations correspond, both in terms of their magnitude and ranking. For the period ending 1 June, the year with the highest (2002) and lowest (2003) runoff corresponded to the years with the highest and lowest SWE respectively (Fig. 7a). For the remaining years, the runoff depth prior to 1 June generally increased with increasing SWE depth (Fig. 7a). For the period ending 1 September, the largest (2007) and smallest (2004) runoff years corresponded to the years with the largest and smallest rainfall, while the magnitude of runoff for the remaining years corresponded with the rainfall depth (Fig. 7b).

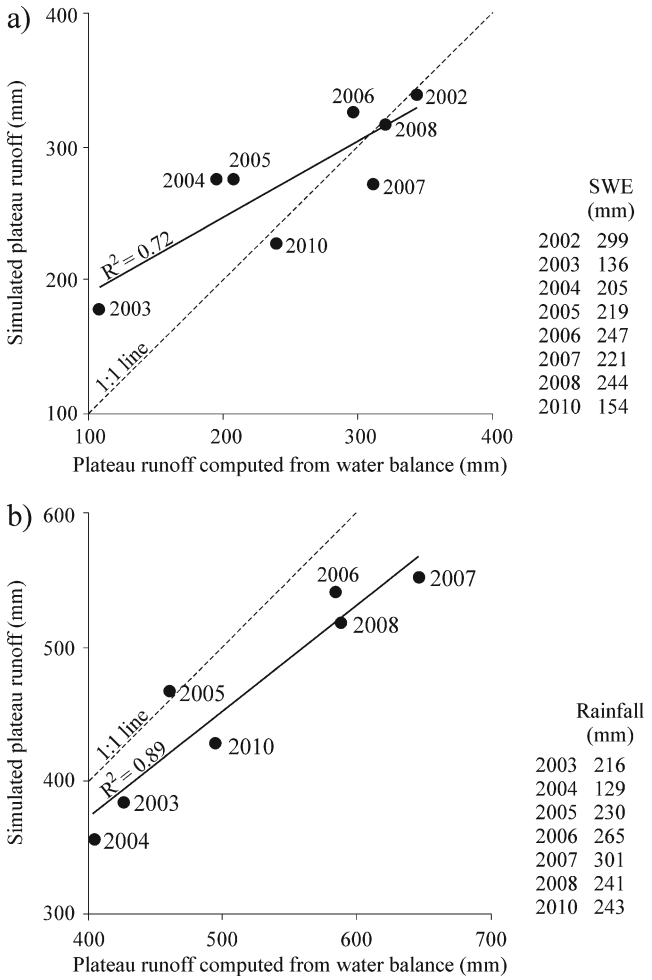


**Fig. 7** The total plateau runoff computed from the water balance (Eq. 1) and simulated using CRHM for each year of study for the period ending **a** 1 June and **b** 1 September. Standardised major axis regression models were **a** Y=0.67X+106.9, $P$=0.008, $R^2$=0.72 and **b** Y=0.84X+31.5, $P$=0.001, $R^2$=0.89

The Y-intercept or elevation of the relationship shown in Fig. 7a differed significantly from 0 (1:1 line: Y=X), while the slope did not differ from 1 ($P$=0.0326 and $P$=0.1098, respectively; based on standardised major axis regression analysis), indicating that, overall, simulated plateau runoff was greater than runoff estimated from the water balance for the period ending on 1 June. Neither intercept nor slope differed from that of unity for the period ending on 1 September (Fig. 7b; $P$=0.6424 and $P$=0.2812, respectively). These differences can be attributed in part to model assumptions of spatial uniformity of active layer thaw. Field observations indicate that early in the thaw season, the depth to the impermeable frost table typically varied by 50 % over short (~1 m) distances, and as a result, areas where the relatively impermeable frost table is close to the ground surface, may obstruct or re-direct subsurface drainage. The assumption of spatial uniformity of thaw depth may in part account for the discrepancy between simulated and computed runoff for the period ending 1 June (Fig. 7a) than in the period ending 1 September (Fig. 7b), since the variation in thaw depth is greater early in the thaw period and as a result so too is the obstruction to subsurface drainage by areas of shallow thaw and the abstraction of drainage into thaw depressions (Wright et al. 2009).

### Influence of permafrost thaw on plateau runoff

The estimates of plateau runoff presented so far do not explicitly account for the influence of permafrost thaw. Permafrost thaw would affect the amount of plateau runoff by (1) lowering the plateau ground surface and therefore the hydraulic gradient driving the subsurface flux, (2) thickening the active layer which would lower the saturated flow zone and therefore the subsurface flow rate by decreasing both the $K_S$ and the hydraulic gradient, and (3) reducing the surface area of the plateau and therefore its runoff producing area. The influence of these thaw-induced changes on the plateau runoff was quantified by re-running the simulations after appropriate changes to the model parameters, and then by comparing the new simulations representing the thawing condition with the original simulations that assumed no permafrost thaw or ground surface subsidence. Three model re-runs were performed for each year so that the effects of the changes to the hydraulic gradient, thaw depth, and runoff producing area could be evaluated independently.

The first simulation re-run (A) concerned the changes to the hydraulic gradient only. The initial simulations assumed a constant hydraulic gradient of 0.019. Re-run A used the hydraulic gradients measured in 1999 (0.019), 2002 (0.018), 2006 (0.015) and 2009 (0.013), and interpolated values for the intervening years and for 2010. Re-run B included the hydraulic-gradient changes represented by re-run A, plus the observed increase of the annual thaw depth. The original simulations assumed an annual maximum thaw depth equal to 0.7 m, which was the depth of the Centre pit excavated and instrumented in

 DOI 10.1007/s10040-012-0935-2

Augus, 2002 on the crest of the plateau (Fig. 1b). Although the temperature record at the Centre pit suggests that the pit thawed more rapidly in the second half of the decade, there were no direct measurements of frost table depth at that location due to concerns of disturbing the buried sensors with the frost probe. According to Fig. 1c, the thaw depth of 0.7 m at the Centre pit in 2002 was greater than the average end-of-summer thaw depth of the measurement transect points until 2005. To account for the affect of the increasing thaw depth, the lowest of the four computational layers defined by the 0.35–0.70 m depth range in the initial run was redefined as 0.35–0.70 m (2006), 0.35–0.73 m (2007), 0.35–0.77 m (2008), 0.35–0.94 m (2010) based on the average end-of-summer thaw depths presented in Fig. 1c. Re-run C included the changes in hydraulic gradient and thaw depth represented by re-run B, plus the observed decrease in plateau surface area. Since the water-flow simulations were made for a 1-m-wide strip, extending from the middle of the plateau to the edge of the fen, only the year-to-year change in the length of this strip had to be specified in order to represent the change in the runoff producing area. The initial simulations assumed a constant strip length of 19.75 m, which is half of the plateau width of 39.5 m measured in 2002. For each year after 2002, re-run C defined the strip length as half of the measured permafrost width presented in Fig. 1c. Interpolated values were used for 2003 and 2007.

The runoff was computed in units of depth (Fig. 8a and b) and volume (Fig. 8c and d). The former illustrates the results of re-runs A and B only, while the volume flux also accounts for the effect of the observed decrease in plateau surface area on drainage. Differences between the re-runs and the initial runs increased year-by-year as the study plateau thawed and subsided. Differences also increased with time within individual years and were therefore greater for the period ending 1 September, since by that time of year, the cumulative drainage was larger, which proportionately increased the difference between the initial and re-run simulations. A summary of the simulation re-runs is given in the following.

*Re-run A.* Model re-run A indicated that the reduction of the hydraulic gradient produced only a small decrease in plateau drainage. For example, for the period ending 1 June 2006, the runoff was only 3 mm lower than that of the initial (i.e. constant-gradient) simulation, representing a volumetric reduction of 0.07 $m^3$ (Fig. 8c); and for the period ending 1 September of that year, it was only 5 mm (Fig. 8b) lower than that of the initial simulation, representing a 0.11 $m^3$ reduction (Fig. 8d). The largest difference between the water flux of the initial simulations and those of re-run were for the period ending 1 September 2008, and amounted to a difference of only 1.5 %. Across years, for the period ending on 1 September there was a small but significant decrease in re-run A runoff compared with unthawed conditions (Table 1).

*Re-run B.* The simulations of re-run B indicated that the reduction in runoff due to increased ground thaw was larger than that resulting from the decreased hydraulic gradient alone. By 2010, the decrease in runoff for the period ending 1 September was 4 mm due to the hydraulic-gradient reduction and 27 mm due to increased thaw, suggesting that the effect of increased thaw depth on runoff is more than six-times greater than that of the hydraulic gradient reduction. However, even the combined effect of increased thaw and decreased hydraulic gradient reduced the runoff of the initial run by 7 % (Fig. 8b). Across years, for the period ending on 1 September, differences between re-run B runoff compared with unthawed conditions were significant only in the summer for both volumetric and total run-off calculations (Table 1).

*Re-run C.* These final runs demonstrated that the year-by-year reduction in the plateau runoff producing area had the largest impact on plateau drainage. For the period ending 1 September 2010, the combined effect of permafrost thaw (i.e. reduced hydraulic gradient, increased thaw depth and loss of runoff producing area) reduced the plateau discharge by 4.0 $m^3$ to approximately half the value (47 %) of the initial run (Fig. 8d). Of this reduction in drainage volume, 3.38 $m^3$ was due to the loss of the plateau surface area. Across years, total runoff was significantly reduced for runs ending in both June and September, while these differences only became apparent for volumetric measures in September (Table 1).

Although Fig. 8 provides some insight into how permafrost thaw reduces the plateau drainage, there are other hydrological consequences of permafrost thaw worth noting. For example, permafrost thaw also changes the temporal pattern of the runoff. The hydrograph peaks of re-run C in the early part of the record (i.e. April and May) rose to only about half the height of those simulated by the initial run (Fig. 9). During the June to August period, when the saturated flow zone (depicted in Fig. 2) occupied the zone of uniformly low $K_S$, the hydrograph rises of re-run C were far more subdued than those of the initial run for that period.

The model simulated the gradual year-to-year change of the ground thaw regime and the effect on the total subsurface drainage. However, changes to the active layer and its thaw regime (Fig. 6) could influence the temporal pattern of plateau runoff. For example, the more gradual thaw regimes of the first 3 years of this study (2002, 2003, 2004) would have kept the subsurface flow zone closer to the ground surface (where $K_S$ is relatively high) for longer periods than in later years, thereby allowing relatively high rates of subsurface flow for extended periods. To investigate the impact of the ground thaw rate on the temporal runoff pattern, the initial simulation for the period ending 1 September 2010 was re-run using the lower thaw rate of 2004. Runoff commenced on 14 April for the initial simulation, but was delayed until 27 April when the 2004 thaw data were used (Fig. 9). The flow rate of the re-run based on 2004 thaw data was also higher but the two rates became indistinguishable by approximately

 DOI 10.1007/s10040-012-0935-2

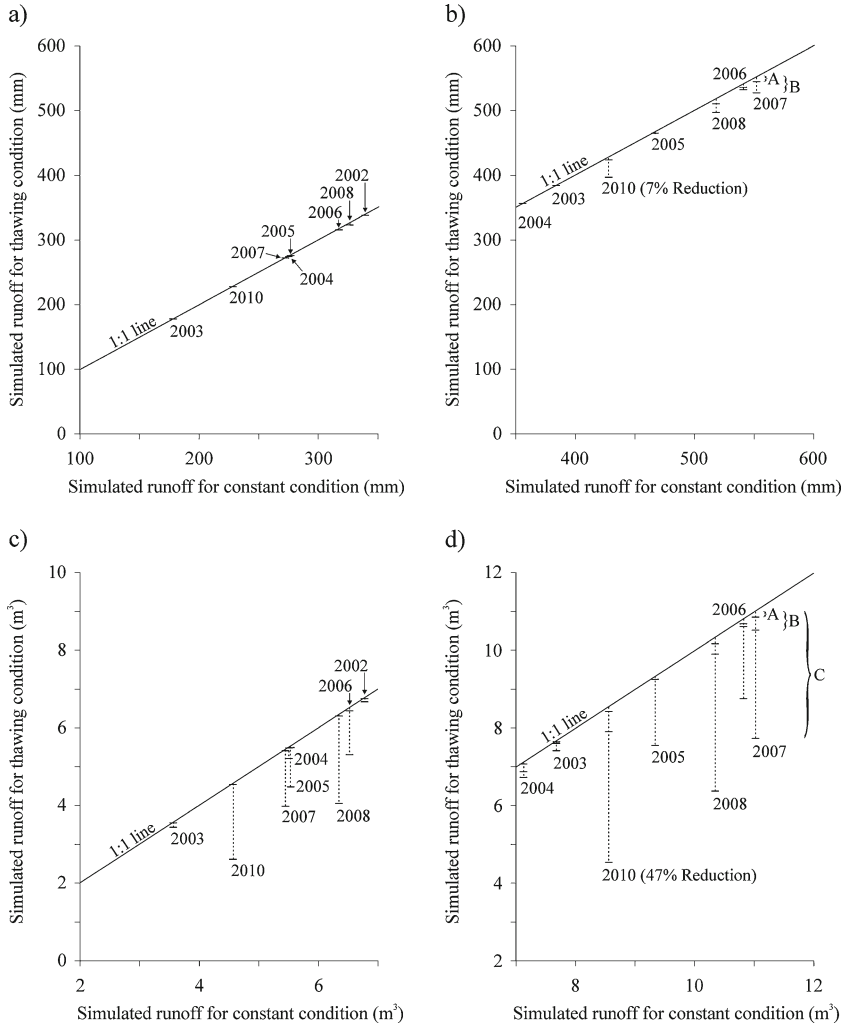


**Fig. 8** Simulated runoff using CRHM for constant conditions of hydraulic gradient, end of summer thaw depth, and plateau surface area defined for the initial CRHM runs in 2002, plotted with the simulated runoff for three conditions that represent the effects on drainage of the permafrost thaw that has occurred since the initial runs. These conditions include the measured decrease in hydraulic gradient (re-run A; represented as *A* in the figure); a decrease in hydraulic gradient and measured increase in end-of-summer thaw depth (re-run B; represented as *B*); the decrease in hydraulic gradient, increase in end-of-summer thaw depth, and measured decrease in plateau surface area (re-run C; represented as *C*). The *1:1 line* indicates the runoff that would occur without any permafrost-thaw-induced changes to drainage. **a** is the total runoff depth for the period ending 1 June; **b** is the total runoff depth for the period ending 1 September; **c** is the total volume flux for the period ending 1 June; and **d** is the total volume flux for the period ending 1 September

**Table 1** Paired *t*-test results comparing unthawed conditions to model re-runs *A*, *B* and *C*. Model re-run A corresponds to a change in hydraulic gradient alone, re-run B includes both change in hydraulic gradient and active layer thickening, while re-run C also includes reduction in peat plateau area. *Spring* and *summer* seasons correspond to model runs which ended on 1 June and those that ended on 1 September, respectively. Asterisks indicate significant differences

| Model re-run | Season | Measurement | *t*-value | *P*-value |
|---|---|---|---|---|
| A | Spring | Volumetric | 1.67 | 0.1395 |
| A | | Total runoff | 1.82 | 0.1114 |
| A | Summer | Volumetric | 3.35 | 0.0150* |
| A | | Total runoff | 4.04 | 0.0068* |
| B | Spring | Volumetric | 1.67 | 0.1395 |
| B | | Total runoff | 1.82 | 0.1114 |
| B | Summer | Volumetric | 2.53 | 0.0446* |
| B | | Total runoff | 3.16 | 0.0196* |
| C | Spring | Volumetric | 1.67 | 0.1395 |
| C | | Total runoff | 3.55 | 0.0093* |
| C | Summer | Volumetric | 2.53 | 0.0446* |
| C | | Total runoff | 3.75 | 0.0095* |

10 July (Julian Day 192), by which time the thaw curves of both 2004 and 2010 were close to or below the bottom of the Centre pit (Fig. 6c). The total discharge by 1 September for the re-run using the 2004 thaw data (8.38 $m^3$) was only slightly lower than for the initial run (8.56 $m^3$) due to the delay in runoff response.

### *Error and uncertainty*

For unfrozen conditions, the accuracy of the water content meters is expected to be ±2 %, as they were calibrated for the peat soils at the study-area plateau. It is difficult to estimate the magnitude of errors associated with deriving the total (i.e. frozen and unfrozen) water in the Centre pit; however, given uncertainties resulting from dividing the Centre pit into computational layers, estimating the position of the freezing front by interpolation from soil temperature data, the assumption of peat saturation below

 DOI 10.1007/s10040-012-0935-2

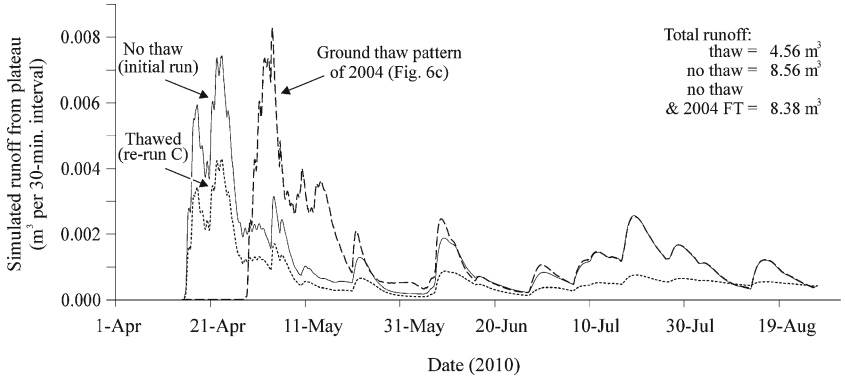


**Fig. 9** Hydrographs from the study plateau simulated using CRHM for 2010. Figure 7b indicates that, relative to the other years, 2010 had an intermediate total runoff by 1 September. Here, the figure shows the hydrograph for *re-run C*, as well as the *initial run*. The hydrograph was produced when the initial simulation for 2010 was re-run using the thaw pattern measured in 2004

the freezing front, and uncertainty regarding over-winter moisture redistribution processes, an error of ±20 % is reasonable. Based on the error estimates of individual water-balance components, and given that some errors may cancel each other over the periods of computation, it was expected that the runoff computed from the water balance may have an error of ±20–30 %. Since neither the water-balance computations nor the CRHM simulations explicitly computed the evaporative flux, and since runoff from the study plateau in 2004 and 2005 was between 2.9 and 4.3 times greater than the evaporative flux (Wright et al., 2005), runoff in the present study may be over estimated by 23–34 %. The large depth-variation of $K_s$ (Fig. 2) introduces additional uncertainty (approximately±20 %) to the CRHM simulations of runoff when the saturated flow zone occupies transition between high and low $K_s$ zones (Fig. 2), since CRHM uses a single average value of $K_s$ to compute flow. Further error may be introduced by the possibility that peat properties such as the hydraulic conductivity may have changed over the study period due to subsidence.

Using a single-instrumented soil pit to derive runoff from water-balance computations introduces uncertainty regarding how well the Centre pit represents the overall plateau. However, as noted in the preceding, the addition of 15 soil pits for 2005 (Wright et al. 2008) indicated very little difference in moisture contents of the Centre pit and the average of the 15 other soil pits. The observed water levels in the Centre pit are plotted, along with model-simulated water level, in Fig. 10 for the years when automated measurements were recorded. The temporal pattern of fluctuations is similar (Fig. 11); however, the simulated water levels were often 10 or more cm below the observed water table. As a result, there were extended periods in each year when CRHM computed runoff using a lower value of $K_s$ (Fig. 2) than expected given the often higher position of the observed water table. However, the seasonal total-runoff values presented for the two computational periods in Fig. 7a and b do not show the simulated runoff to be persistently lower. Figure 10b plots the average and range of water-table depths measured at the additional 15 soil pits used in 2005. The data for the sample of 5 days plotted in the figure indicates that, for the most part, both the simulated and observed water tables fall within the range of observed water-table depths measured at the 15 soil pits throughout the plateau. Figure 11 uses 2004 for a more detailed comparison of CRHM simulations compared with field observations. The simulated snowmelt and thaw curves for each year matched closely with the measured values, since they were computed using temperature index coefficients determined by trial and error until a good match was obtained.

## Conclusions and recommendations

The total moisture content in the upper 0.4 m of the active layer increased during winter months and was greatest at 0.1 m, where the average over-winter increase for the 2001–2010 period was 0.34 per volume ($\sigma$=0.09). This migration of moisture toward the 0.1-m-depth position during winter produces a zone of high ice-content near the ground surface, a process that appears to prime the active layer for rapid transmission of water early in the thaw period when the snowmelt water supply is large and the water table perched above the relatively impermeable frost table occupies the zone of uniformly high $K_S$.

On average, over the 2001–2010 study period, ground freezing and thawing commenced at a FPD of ~−0.3 °C at the −0.3 m depth. Regardless of the moisture content prior to freezing, it decreased to a constant of ~0.2 per volume as the soil temperature lowered to −0.7 °C. For each year of study, two distinct levels of unfrozen moisture were evident for the 0.7-m-deep Centre pit: a ~4-month winter minimum period when soil temperatures were below −0.7 °C throughout the profile, and the unfrozen moisture content was relatively constant at 120 mm; and a summer level when the entire 0–0.7 m profile was thawed and the depth of unfrozen moisture

 DOI 10.1007/s10040-012-0935-2

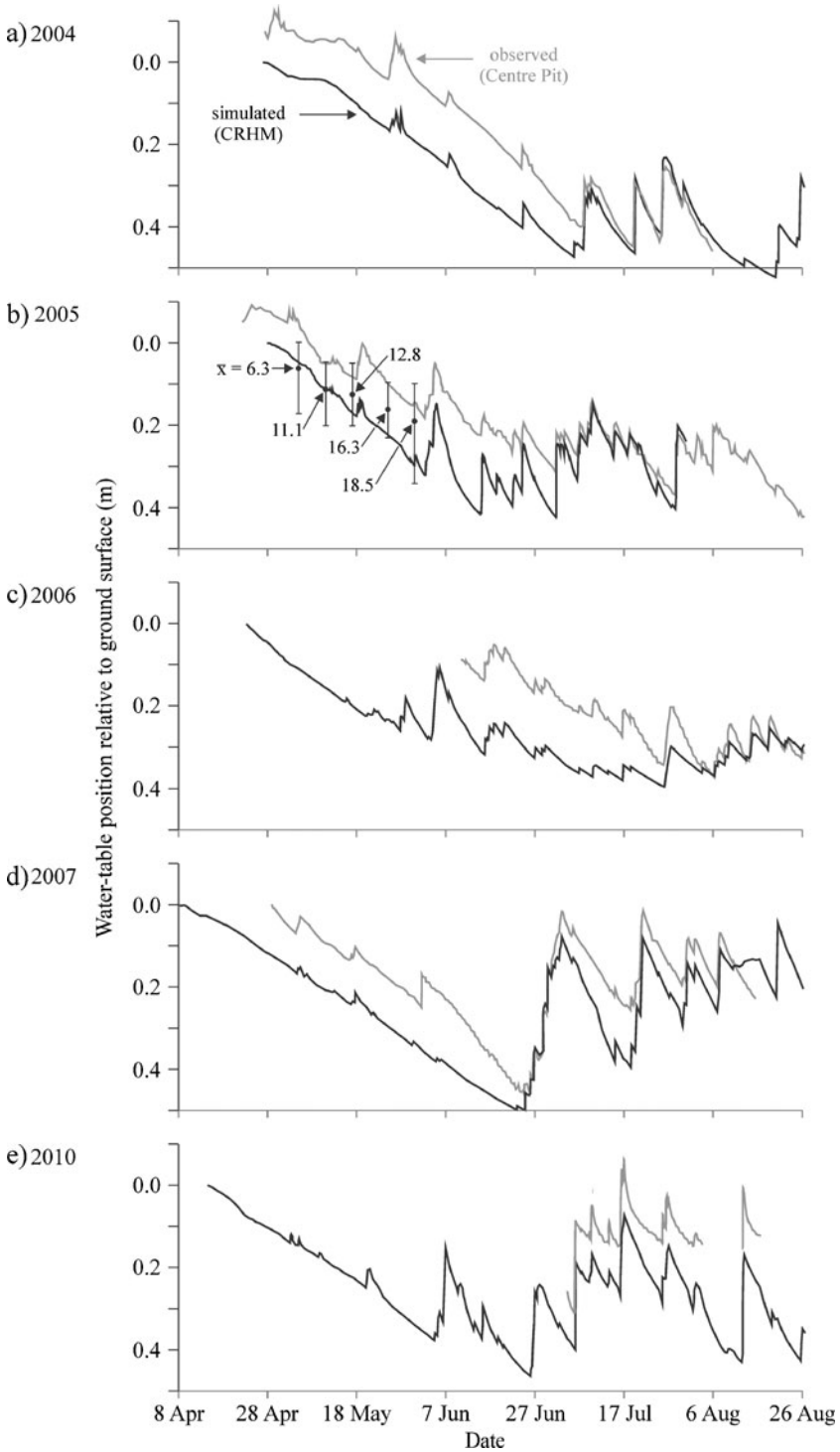


**Fig. 10** Observed (*Centre pit*) and simulated (*CRHM*) water tables for the years when measurements were recorded. For 2005 (**b**), the range and average water-table depths of the 15 additional wells are plotted for ~5-day intervals

in the profile ranged between 370 and 430 mm. The profile was in transition between the two moisture regimes during the thawing and freezing zero-curtain periods. The duration of the zero curtain periods increased with depth, and for the autumn of 2003, it ranged from 20 days at 0.05 m to 90 days at 0.7 m; during soil thawing in 2004, the zero curtains lasted between 8 days at 0.05 m and 65 days at 0.7 m.

The runoff response of a plateau depends on which of the three zones of $K_S$ the water table is displaced into. This in turn depends on the magnitude of input, the water-table depth position prior to the input, and the drainable porosity at that depth. A rapid runoff response is generated if the water table is displaced into the zone of uniformly high $K_S$. There is evidence that permafrost thaw has

 DOI 10.1007/s10040-012-0935-2

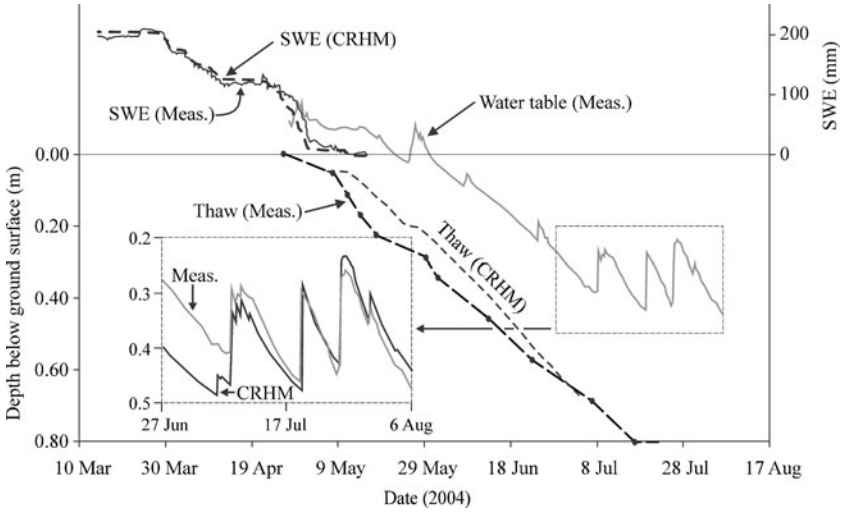


**Fig. 11** Observed (Centre pit) and simulated (*CRHM*) snow-water equivalent (*SWE*) depth, thaw depth and water-table position for a period in the summer of 2004

affected the hydraulic response of the peat plateau. For example, the moisture and temperature of the active layer steadily rose with each year since monitoring began in August 2001. The largest increase in liquid-moisture content was at 0.1 m, where at the time of freeze-up, the moisture content increased from 0.32 in 2001 to 0.54 in 2010. This suggests a greater time requirement to freeze the active layer in the fall and to thaw it in the spring. However, in spite of this, thaw of the 0.1–0.4- m-depth range occurred about 20 days earlier by the final year of the study than in 2002, suggesting greater energy availability for thaw, greater thermal conduction of the upper active layer, or both. Earlier thaw of the active layer affects plateau runoff, since the frost table (and therefore the subsurface flow zone) would fall below the zone of uniformly high $K_S$ earlier in the thaw period, and, therefore, a greater magnitude of input would be required to raise the water table back into the high $K_S$ zone and generate a rapid runoff response. However, such a condition would be relatively short-lived if permafrost thaw continues to the point that the plateau is transformed into a wetland (i.e. bog or fen), since the water table in wetlands remains at or near the ground surface.

Permafrost thaw reduced runoff from the peat plateau by (1) lowering the hydraulic gradient driving the subsurface flux, (2) thickening the active layer, and most importantly by (3) reducing the surface area of the plateau. By 2010, the cumulative permafrost thaw had reduced the plateau efflux to 47 % of what it would have been had there been no change in hydraulic gradient, active layer thickness and plateau surface area since 2002.

**Acknowledgements** We wish to acknowledge the financial support of the Natural Sciences and Engineering Research Council, and the Canadian Foundation for Climate and Atmospheric Sciences (*IP3* Research Network, and *PET* Research Partnership). We also acknowledge the logistical support provided by the National Water Research Institute (Saskatoon) and by Mr. Gerry Wright and Mr. Roger Pilling of the Water Survey of Canada (Fort Simpson). The Aurora Research Institute is gratefully acknowledged for its assistance in obtaining a research license. We also wish to thank the Denedeh Resources Committee, Deh Cho First Nation, Fort Simpson Métis Local No. 52, Liidlii Kue First Nation and the Village of Fort Simpson for their support of this project. In particular, we thank Mr. Allan Bouvier and Mr. Allen Bonnettrouge of the LKFN. Dr. Masaki Hayashi of the University of Calgary is also acknowledged for many insightful discussions on hydrological processes at the study site, and for his analysis of the frozen peat core samples. Mr. Tom Brown of the Centre for Hydrology, University of Saskatchewan is thanked for developing the computer code for the runoff module in CRHM. The authors wish to thank the three anonymous reviewers and Professor C. Burn for their helpful suggestions. We also wish to thank the Guest Editor, Professor M-K (Hok) Woo for his helpful suggestions.

## References

Arain MA, Black TA, Barr AG, Griffis TJ, Morgenstern K, Nesic Z (2003) Year-round observations of the energy and water vapour fluxes above a boreal black spruce forest. Hydrol Process 17: 3581–3600

Aylesworth JM, Kettles IM (2000) Distribution of fen and bog in the Mackenzie Valley, 60°N–68°N. Geol Surv Can Bull 547, Natural Resources Canada, Ottawa

Beilman DW, Robinson SD (2003) Peatland permafrost thaw and landform type along a climate gradient. In: Phillips M, Springman SM, Arenson LU (eds) Proceedings of the Eighth International Conference on Permafrost, vol. 1. Balkema, Zurich, pp 61–65

Carey SK, Woo M-K (2000) Within slope variability of ground heat flux, subarctic Yukon. Phys Geogr 21:407–417

Childs EC (1971) Drainage of groundwater resting on a sloping bed. Water Resour Res 7:1256–1263

Dingman SL (2002) Physical hydrology, 2nd edn. Prentice Hall, Englewood Cliffs, NJ, 646 pp

Hamlin L, Pietroniro A, Prowse T, Soulis R, Kouwen N (1998) Application of indexed snowmelt algorithms in a northern wetland regime. Hydrol Process 12:1641–1657

Hayashi M, Goeller N, Quinton W, Wright N (2007) A simple heat-conduction method for simulating the frost-table depth in hydrological models. Hydrol Process 21:2610–2622

Hegginbottom JA, Radburn LK (1992). Permafrost and ground ice conditions of northwestern Canada. Geological Survey of Canada Map 1691A, scale 1:1 000 000, GSC, Ottawa

Hoag RS, Price JS (1997) The effects of matrix diffusion on solute transport and retardation in undisturbed peat in laboratory columns. J Contam Hydrol 28(3):193–205

Johannessen OM, Bengtsson L, Miles MW, Kuzmina SI, Semenov VA, Alekseev GV, Nagurnyi AP, Zakharov VF, Bobylev LP,

Pettersson LH, Hasselmann K, Cattle HP (2004) Arctic climate change: observed and modelled temperature and sea-ice variability. Tellus Series A: Dynamic Meteorol Oceanogr 56:328–341

Jorgenson MT, Osterkamp TE (2005) Response of boreal ecosystems to varying modes of permafrost degradation. Can J For Res 35:2100–2111. doi:10.1139/X05-153

Jorgenson MT, Romanovsky V, Harden J, Shur Y, O'Donnell J, Schuur EAG, Kanevskiy M, Marchenko S (2010) Resilience and vulnerability of permafrost to climate change. Can J For Res 40(7):1219–1236. doi:10.1139/X10-060

Kwong J, Gan T (1994) Northward migration of permafrost along the Mackenzie Highway and climate warming. Clim Change 26:399–419

Lafleur PM, Schreader CP (1994) Water loss from the floor of a subarctic forest. Arct Alp Res 26:152–158

Lantz TC, Kokelj SV (2008) Increasing rates of retrogressive thaw slump activity in the Mackenzie Delta region, N.W.T., Canada. Geophys Res Lett 35:L06502

Meteorological Service of Canada (MSC) (2011) National climate data archive of Canada. Environment Canada, Dorval, QB

National Wetlands Working Group (NWWG) (1988) Wetlands of Canada: ecological land classification series, no. 24. Sustainable Development Branch, Environment Canada, Ottawa, and Polyscience Publ., Montreal, 452 pp

Pomeroy JW, Gray DM, Brown T, Hedstrom NR, Quinton WL, Granger RJ, Carey S (2007) The cold regions hydrological model, a platform for basing process representation and model structure on physical evidence. Hydrol Process 21:2650–2667

Priestley CHB, Taylor RJ (1972) On the assessment of surface heat flux and evaporation using large-scale parameters. Monthly Weather Rev 100(2): 81–92

Quinton WL, Gray DM (2003) Subsurface drainage from organic soils in permafrost terrain: the major factors to be represented in a runoff model. Refereed Proceedings of the 8th International Conference on Permafrost, Davos, Switzerland, July 2003, 6 pp

Quinton WL, Hayashi M (2007) Recent advances toward physically-based runoff modeling of the wetland-dominated, Central Mackenzie River Basin. Cold Region Atmospheric and Hydrologic Studies. In: Woo M-K (ed) The Mackenzie GEWEX experience, vol 2: hydrological processes. Springer, Heidelberg, Germany, pp 257–279

Quinton WL, Gray DM, Marsh P (2000) Subsurface drainage from hummock covered hillslopes in the Arctic Tundra. J Hydrol 237:113–125

Quinton W, Hayashi M, Pietroniro A (2003) Connectivity and storage functions of channel fens and flat bogs in northern basins. Hydrol Process 17:3665–3684

Quinton WL, Carey SK, Pomeroy JW (2005) Soil water storage and active-layer development in a sub-alpine tundra hillslope, southern Yukon Territory, Canada. Permafrost Periglacial Process 16:369–382

Quinton WL, Hayashi M, Carey SK (2008) Peat hydraulic conductivity in cold regions and its relation to pore size and geometry. Hydrol Process 22:2829-2837. doi:10.1002/hyp.7027

Quinton WL, Hayashi M, Chasmer LE (2011) Permafrost-thaw-induced land-cover change in the Canadian subarctic: implications for water resources. Hydrol Process (Scientific Briefing) 25:152–158. doi:10.1002/hyp.7894

Rawlins M, Ye H, Yang D, Shiklomanov A, McDonald KC (2009) Divergence in seasonal hydrology across northern Eurasia: emerging trends and water cycle linkages. J Geophys Res 114: D18119. doi:10.1029/2009JD011747

Robinson SD, Moore TR (2000) The influence of permafrost and fire upon carbon accumulation in high boreal peatlands, Northwest Territories, Canada. Arct Antarct Alp Res 32:155–166

Rowland JC, Jones CE, Altmann G, Bryan R, Crosby BT, Geernaert GL, Hinzman LD, Kane DL, Lawrence DM, Mancino A, Marsh P, Mcnamara JP, Romanovsky VE, Toniolo H, Travis BJ, Trochim E, Wilson CJ (2010) Arctic landscapes in transition: responses to thawing permafrost. Eos 91(26):229. doi:10.1029/2010EO260001

Smith MW, Riseborough DW (2002) Climate and the limits of permafrost: a zonal analysis. Permafrost Periglacial Process 13:1–15

St. Jacques JM, Sauchyn DJ (2009) Increasing winter baseflow and mean annual streamflow from possible permafrost thawing in the Northwest Territories, Canada. Geophys Res Lett 36:L01401

van Genuchten MT (1980) A closed-form equation for predicting the hydraulic conductivity of unsaturated soils. Soil Sci Soc Am J 44:892–898

Thie J (1974) Distribution and thawing of permafrost in the southern part of the discontinuous permafrost zone in Manitoba. Arctic 27:189–200

Woo M-K (1986) Permafrost hydrology in North America. Atmos Ocean 24(3):201–234

Wright N, Quinton WL, Hayashi M (2008) Hillslope runoff from ice cored peat plateaus in a discontinuous permafrost basin, Northwest Territories, Canada. Hydrol Process 22:2816–2828

Wright N, Hayashi M, Quinton WL (2009) Spatial and temporal variations in active layer thawing and their implication on runoff generation in peat-covered permafrost terrain. Water Resour Res 45:W05414

Zoltai SC (1993) Cyclic development of permafrost in the peatlands of northwestern Alberta, Canada. Arct Alp Res 25:240–246